remote sensing

MDPI

Review

Applications of Unmanned Aerial Systems (UASs) in Hydrology: A Review

Mercedes Vélez-Nicolás [1,*], Santiago García-López [1], Luis Barbero [1], Verónica Ruiz-Ortiz [2] and Ángel Sánchez-Bellón [1]

[1] Department of Earth Sciences, Faculty of Marine and Environmental Sciences, University of Cádiz, 11510 Puerto Real, Spain; santiago.garcia@uca.es (S.G.-L.); luis.barbero@uca.es (L.B.); angel.sanchez@uca.es (Á.S.-B.)

[2] Department of Industrial and Civil Engineering, Higher Polytechnic School of Algeciras, University of Cádiz, 11202 Algeciras, Spain; veronica.ruiz@uca.es

* Correspondence: mercedes.velez@uca.es

Abstract: In less than two decades, UASs (unmanned aerial systems) have revolutionized the field of hydrology, bridging the gap between traditional satellite observations and ground-based measurements and allowing the limitations of manned aircraft to be overcome. With unparalleled spatial and temporal resolutions and product-tailoring possibilities, UAS are contributing to the acquisition of large volumes of data on water bodies, submerged parameters and their interactions in different hydrological contexts and in inaccessible or hazardous locations. This paper provides a comprehensive review of 122 works on the applications of UASs in surface water and groundwater research with a purpose-oriented approach. Concretely, the review addresses: (i) the current applications of UAS in surface and groundwater studies, (ii) the type of platforms and sensors mainly used in these tasks, (iii) types of products generated from UAS-borne data, (iv) the associated advantages and limitations, and (v) knowledge gaps and future prospects of UASs application in hydrology. The first aim of this review is to serve as a reference or introductory document for all researchers and water managers who are interested in embracing this novel technology. The second aim is to unify in a single document all the possibilities, potential approaches and results obtained by different authors through the implementation of UASs.

Keywords: drone applications; surface water; groundwater; photogrammetry; optical sensing; thermal infrared

Citation: Vélez-Nicolás, M.; García-López, S.; Barbero, L.; Ruiz-Ortiz, V.; Sánchez-Bellón, Á. Applications of Unmanned Aerial Systems (UASs) in Hydrology: A Review. *Remote Sens.* **2021**, *13*, 1359. https://doi.org/10.3390/rs13071359

Academic Editor: Giacomo De Carolis

Received: 25 February 2021
Accepted: 31 March 2021
Published: 1 April 2021

1. Introduction

Sustainable water management has become a major concern over the past decades; as water demand increases with socioeconomic development and population growth, the availability of freshwater resources shrinks due to climate change, aquatic ecosystem degradation and anthropogenic impacts. According to UNESCO [1], water use has been increasing 1% annually worldwide since the 1980s and the global demand for water is expected to keep a similar trend until 2050. This would account for an increase of 20% to 30% above the current level of water use. Under these circumstances, ensuring water in adequate quantity and quality to meet food security, environmental targets, public health requirements and the production of energy, services and other goods remains one of the greatest challenges for water managers in coming years. This is especially critical in regions such as sub-Saharan Africa, central and southwest Asia, which are affected by persistent multi-year droughts, or the Mediterranean basin, where water resources are unevenly distributed and present severe deficiencies in its southern and eastern parts. On the other side of the coin, extreme precipitation events and alterations in flood frequency and duration are affecting an increasing number of countries globally, causing loss of lives, health-related issues and multiple social and economic damages. These extreme

hydrological phenomena are likely to be exacerbated as a result of climate change, with increases in their frequency according to the Fifth Assessment Report of the IPCC [2]. Likewise, water quality issues are becoming a major concern. Numerous aquatic systems have undergone severe pollution processes linked to agricultural, domestic and industrial activities and waste disposal, situation that compromises the supply of clean potable water and have deleterious effects on the ecosystem functioning and biota.

This scenario demands effective management and intervention in catchments, which necessarily involves gaining further knowledge of hydrological systems and filling current information gaps. In this regard, unmanned aerial systems (UAS) also known as unmanned aerial vehicles (UAVs), remotely piloted aircraft systems (RPAS) or drones, have recently emerged as new allies in environmental monitoring and management. UAS have not only made bird's eye observation a reality, but also offer a vast range of applications that is continually growing as technology advances. Although initially devised to support military operations, the civilian and scientific applications of UAS have attracted increasing attention in recent years, experiencing an exponential growth in their commercial, governmental and amateur use. The advances in fabrication, remote control capabilities and power systems along with the improvements in sensing technologies installed onboard, have led to the development of a wide range of UAS that can be used to obtain valuable information in different contexts. Numerous advantages of UASs over other systems can be cited; they are portable and enable the retrieval of data with very-high spatial resolutions and unprecedent temporal coverage. They also enable engagement with areas that would otherwise be inaccessible or cost-prohibitive, especially if compared with methods such as airborne campaigns. Moreover, these platforms are easy to deploy, can be flown in small enclosed areas [3] and their imagery might constitute systematic and permanent data that can be used by other individuals and organizations [4]. Regarding the latter aspect, it should be noted that there is still a long way to go in terms of standardization of the methods and available information. To date, UASs have been implemented in a wide range of fields, such as wildlife research and monitoring [5,6] forestry [7,8], precision agriculture [9], architecture, engineering and construction [10,11], disaster management [12] and social research just to name a few.

The need for monitoring the elements of the hydrological cycle is a widely recognized issue. Although in the last decades the field of hydrology has witnessed tremendous advances that have resulted in an increasing number of papers on the subject, as McCabe et al. [13] pointed out, there are still significant gaps in our hydrological knowledge and analysis capabilities such as the estimation of water and mass transport processes across aquatic–terrestrial interfaces, groundwater depth and storage, deep soil moisture, evaporation or snow water equivalent, among others. In this regard, the emergence of UAS is leading to improvements in the understanding of hydrological processes and the management of water resources [14].

This article presents a review focused on the latest applications and advances of UAS technology in the field of hydrology, concretely in water resource research, comprising surface water and groundwater. Although there are other reviews in this field, some have a general scope, addressing the application of UAS to a wide range of civilian and environmental purposes [15] while others focus on very specific aspects of hydrology. For instance, Carrivick and Smith [16] reviewed the application of the structure from motion (S*f*M) algorithms in photogrammetry for aquatic and fluvial environments, Tomsett and Leyland [17] the current applications of remote sensing in river corridors and Rhee et al. [18] the application of UAS remote sensing to fluvial environments exclusively. DeBell et al. [14] focused on pragmatic concepts of UAS technology and sensors adequate for water resource management. Several authors reviewed the applications of UAS in harmful algal bloom studies [19,20]. Here, nevertheless, we address the vast range of UASs applications in inland water bodies with a purpose-oriented approach, classifying them according to the aim of the research conducted. This paper addresses (i) the current applications of UAS in surface and groundwater research, (ii) the type of UASs and sensors

mainly used in these tasks, (iii) the type of products generated from UAS-borne data, (iv) the advantages and limitations associated with their use and (v) knowledge gaps and future prospects of UASs application in freshwater research and management. Studies on oceanic-coastal applications, hydric erosion, atmospheric water cycle, glaciology and aquatic biodiversity/ecology were excluded from this review.

2. Methodology

An exhaustive search of papers published in academic journals was carried out from August to November 2020. Papers without direct relevance to the use of UAS in freshwater research were discarded. The academic databases and search engines used were Scopus, Google Scholar, Science Direct and Web of Science. Search results were restricted to English language. Table 1 depicts the keywords used in the bibliographic search, including drone-related and hydrology-related terms.

Table 1. Search terms.

UAS and Sensor-Related Terms		Hydrology-Related Terms	
Drone LiDAR Remote sensing RPAS UAS UAV Unmanned Aerial System Unmanned Aerial Vehicle Structure from Motion RGB	Photogrammetry Multispectral Hyperspectral Thermal infrared	Algal bloom Aquifer Bathymetry Flooding Freshwater Groundwater Hydrology Morphology River River discharge Riverine plastic Runoff	Submarine groundwater discharge Subsidence Surface velocity Surface-Groundwater interaction Thermal plume Thermal structure Water budget Water level Water pollution Water sampling Water storage Water table Wetland

For each application covered in this paper, search was conducted using different combinations of keywords, such as: "UAS hydrology"; "unmanned vehicle bathymetry"; "river bathymetry UAV"; "UAV river discharge"; "water surface velocity UAV", "algal bloom UAV", "UAS submarine groundwater discharge", etc.

Only those papers published over the last two decades (2000–2020) were considered in order to report the most updated information and ensure the inclusion of the most relevant works, given the recent development of this technology.

The study focuses on the applications of UASs in hydrology, concretely in freshwater research, thus the literature search process was restricted to those experiences in which UAS were used to study rivers, lakes, reservoirs, wetlands, groundwater bodies and the interactions among them. Figure 1 shows the steps followed in the literature search and classification process, from the initial screening and selection of eligible articles to their final inclusion. Research articles were manually screened by reading the title and abstract, and to ensure relevance, were subsequently analyzed in detail. After discarding duplicates and non-relevant works, a total of 122 research papers were selected and subsequently categorized according to the focus of the research work (Surface-groundwater interactions, water levels, contamination studies, system dynamics, etc.). It should be noted however, that some of the UAS applications presented here could fit into more than one category. For this reason, the papers have been classified according to the main objective of the study.

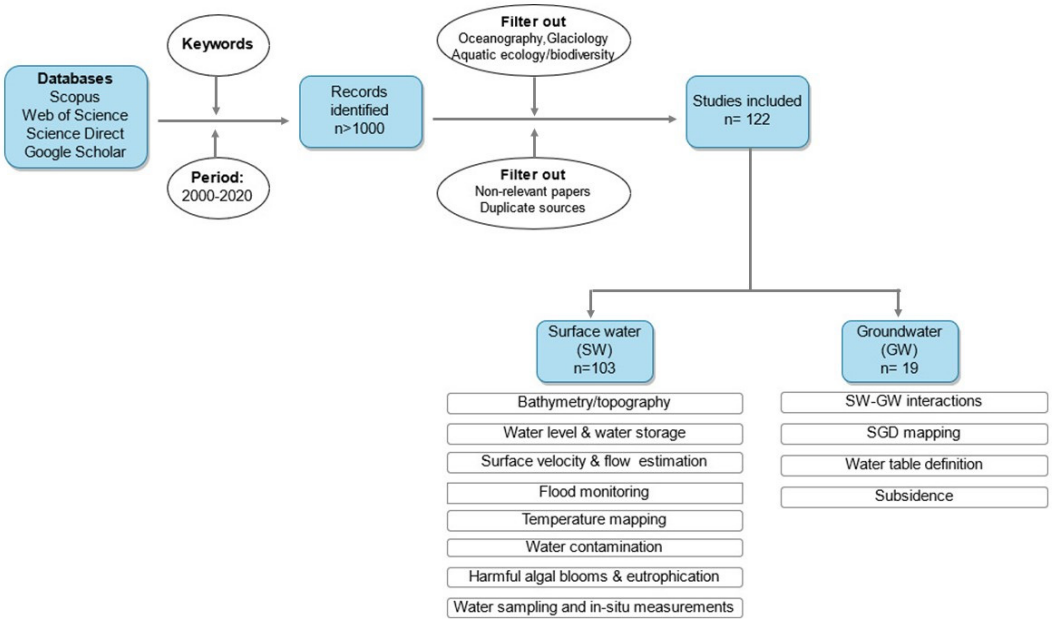

Figure 1. Process of literature search and classification.

3. Types of UAS, Sensors and Other Payloads

3.1. Platforms

These sections do not intend to make an exhaustive overview on the type of UAS, sensor, power systems, etc., but to provide the necessary background for the comprehension of the review as a whole. The vehicle itself is just one part of the complete unmanned aerial system as recognized by other authors [21]. Components such as the control and command element, the payload, take off and recovery system, data link and transmission, and the most important part: the human component, are essential for the system to perform its task.

An unmanned aerial system consists of a flying device that includes: (i) A platform with the structural, mechanical and electronic elements necessary for the flight, its control and stability, (ii) a set of sensors and devices for the acquisition of information from the environment and (iii) a ground control station. UAS characterization can be made based on different variables. Normally, they are classified based on weight [22,23]. Terms such as "nano drone", "micro drone", "mini drone", "pico-drone", etc., are the most frequently used. Apart from weight, other authors include in the classification the typology of aerial vehicle itself or the take-off and landing mode: horizontal take-off and landing (HTOL) versus vertical take-off and landing (VTOL) [24]. Unconventional UAS such as bio-drones, smart dust, air-land-water hybrid drones are being considered in recent times [24]. In any case, most of the applications discussed in this work refer to "lightweight UAS", which due to their reduced maximum take-off weight (MTOW) (less than 7 kg), affordable price, easy deployment and high performance are widely used in scientific research. The most affordable models range between 500 and 1500 €, while the most sophisticated can reach prices up to 120,000 € including the sensing equipment. Although some authors such as Watts et al. [25] propose a classification for civil applications that ranges from very small UAS to large remotely controlled vehicles that can reach thousands of meters in height and many hours of autonomy, legal restrictions in most countries justify a more restrictive classification. DeBell et al. [14], classified the lightweight UASs and analyzed their main characteristics and the available sensors with application to the management of water resources. More recently, Johnston [26] established a new classification and provided a current overview of platforms and sensors that, although it is oriented at marine research and conservation, it is also of interest for research on water resources.

In general, for most hydrological applications these platforms can be categorized according to their airframe configuration, propulsion method, and flight characteristics into four main types: multi-rotor, fixed wing, transitional and others (balloons, kites and blimps). Multi-rotor UASs have multiple engines and propellers that allow the lift, movement and orientation of the platform (pitch, roll, and yaw). Multi-rotors, also known as multicopters, typically employ four (quadcopter), six (hexacopter), or eight (octocopter) motors and propellers; by increasing or decreasing the output of individual motors it is possible to control the movement of such vehicles. A greater number of motors, especially in larger UASs, reduces the risk of falling due to mechanical failures, even though this redundancy is often accompanied by a reduction in efficiency. In fact, the main limitation of multirotor systems is their flight time, mostly due to higher energy demands, battery weight and energy storage constraints. Finally, these types of UASs are manufactured from lightweight and resistant materials such as aluminum, composites (carbon fiber) and plastic.

Fixed-wing UASs have one or two wings that provide maneuverability and lift; they can have several wings configurations (gliders, delta wings, canards, among others). Fixed-wing UASs are generally driven by one or two motors and propellers in a push or pull configuration. These types of UASs are manufactured from very lightweight materials, including various forms of expanded foam (polyolefin, polypropylene or polystyrene) and composite. The flight efficiency of these aircraft is usually higher than in the multi-rotors UASs, due to their lower relative weight and the fact that the lift is of the passive type, through large airfoil surfaces.

Transitional UASs combine aspects of multi-rotor and fixed-wing devices to provide greater flexibility in their use. They intend to incorporate the advantages of the vertical take-off and landing of the former with the greater autonomy and range of action of the latter. Vertical flight is typically driven through three or four motors facing upward, and horizontal flight is driven by a motor and propeller in a push configuration while lift is produced by the wings.

Finally, the category "other" includes devices that either do not have autonomous means of propulsion (kites and balloons) or, if they do, the lift is given by gas lighter than air (blimps). In recent years, these devices have been gradually replaced in most applications by the previous types, due to technological development which have notably improved their performance. Table 2 shows the main characteristics of the platform classes and Figure 2 illustrates different types of platforms and sensors.

Albeit different power supply and energy management systems can be used (see a review on this topic in [27]) most UASs used for research purposes are battery powered. Lithium polymer batteries provide significant energy density and can discharge enough electrical current to meet the variable electrical current demands of the engine and payload. Some systems are hybrid, employing combustion engines together with battery-powered electric motors.

The flight control system, sometimes named autopilot, is the core of the vehicle. It normally includes a flight control processing unit composed of an inertial measurement unit (IMU), electronic speed control (ESC) units, barometer and a global navigation satellite system (GNSS). The IMU consists of a set of accelerometers (normally 3), gyroscopes and magnetometers whose main purpose is determining the orientation, linear and angular accelerations to estimate the movement direction with respect to the earth magnetic field. A data storage system and communication modules (telemetry) are also additional parts of the flight control system. UASs rely on two main navigation technologies, Inertial Navigation Systems (INS) and Global Navigation Satellite Systems (GNSS), so that they can work in a GNSS-only or INS/GNSS coupling mode. The cost reduction and miniaturization of high-performance GNSS units, which allow connection to a nearby reference station and reception of correctional data in real time (kinematic correction), can provide accuracies of 3–5 cm in the dynamic position of the platform, with the consequent improvement in the observations made using sensors and devices.

Table 2. Classification of lightweight unmanned aerial systems (UAS) platforms and their main characteristics.

Main Features	Multi-Rotor	Fixed-Wing	Transitional	Other (Balloons, Kites and Blimp)
Diameter or wing-span	35–150 cm	100–200 cm	100–200 cm	Up to 5 m
Flight time	15–50 min	25–75 min	25–90 min	Hours
Payload Capability	1–2.5 kg	1–2 kg	1–2 kg	>2.5 kg
Maneuverability	High	Medium	Medium-high	Low
Wind resistivity	10–15 m/s	8–20m/s	12 m/s	Highly variable
Ability to fly under windy conditions	Medium	Medium-high	Medium-high	Low
Spatial coverage in a single flight	20–40 ha	80–320 ha	80–320 ha	Variable
Expertise required	Low	Medium	High	Low
Take-off and landing capability	Vertical take-off and landing (VTOL)	Launch line, catapult, or hand launch; open area for landing or parachute	Vertical take-off and landing (VTOL)	Vertical take-off and landing (VTOL)
Velocity or thrust failure	Crash	Glide capability, controlled crash, or parachute	Glide capability, controlled crash, or parachute	Variable
Ability to carry sampling devices	Yes	No	No	No

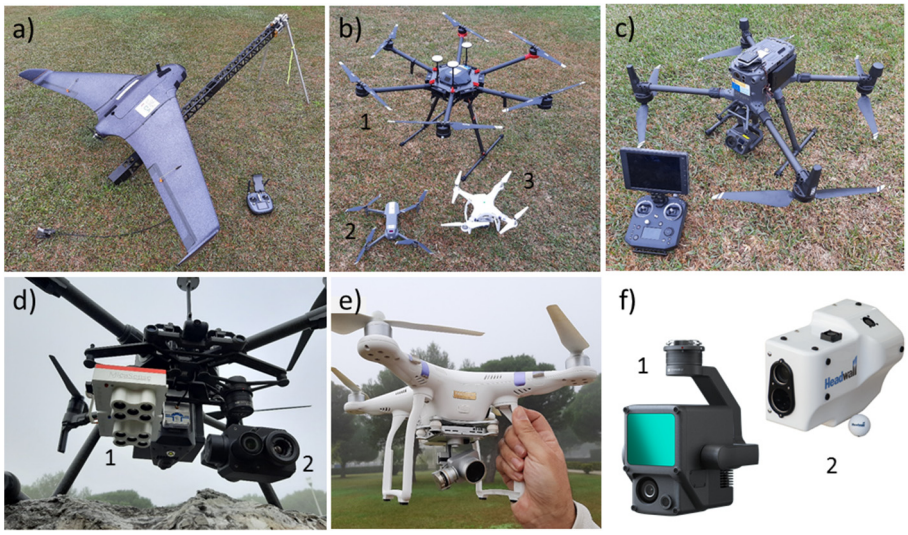

Figure 2. (**a**) Fixed wing UAS Atyges-FV1 on catapult; (**b**) 1. Hexacopter DJI Matrice 600 pro, 2. Micro UAS Quadcopter DJI Mavic Pro, 3. Micro UAS Quadcopter DJI Phantom 3 professional; (**c**) Quadcopter DJI Matrice 300 RTK and radiocontrol station; (**d**) 1. Multispectral camera Micasense dual (10 bands) and 2. visible and thermal camera Zenmuse XT2 onboard a DJI Matrice 210 RTKv2; (**e**) RGB camera Sony EXMOS onboard a DJI Phantom 3 professional; and (**f**) 1. LiDAR DJI Zenmuse L1 and 2. hyperspectral camera Headwall VNIR-SWIR. Courtesy of the Drone Service of the University of Cádiz.

3.2. Sensors and Other Payloads

The application of UASs in hydrology fundamentally encompasses the field of low altitude aerial Photogrammetry and Remote Sensing (PaRS), although other non-remote applications have also been successfully developed. In any case, an important limitation of

these systems is the size and weight of the payload, especially in lightweight UASs, which rarely exceed 2.5 kg. This implies that the sensors and devices included in the UAS must meet special requirements in terms of lightness and packaging. Fortunately, in recent years a substantial number of sensor systems for PaRS applications that meet these conditions have been specifically developed by manufacturers to be mounted in lightweight UAS. Most of the sensors used in hydrological UAS-based mission are essentially digital cameras, which are optical-electronic sensors. These sensors consist of an optical system (lens) that captures and projects electromagnetic radiation onto a CCD (Charge Coupled Device) or alternatively onto a CMOS (Complementary Metal-Oxide-Semiconductor) device, so that the light generates in each element of a matrix an electrical current that is registered and encoded. Currently, there is a wide range of passive optical-electronic sensors available for UAS, which covers a wide spectrum range (400–14,000 nm) and includes RGB, multispectral, hyperspectral and thermal infrared (TIR) cameras.

The usefulness of RGB cameras, which record radiation in the visible spectrum, lies in obtaining aerial videos and imagery that can be processed to orthorectified image mosaics and digital surface models (DSM) using photogrammetry Although some models already exist, usually RGB cameras onboard UAS are non-metric, which implies that the interior orientation elements (focal length, principal point location, distortion parameters, etc.) have not been determined through a calibration process, in addition to not meeting certain requirements for lens quality and dimensional stability of its components. This aspect, which constitutes a serious drawback for stereoscopic photogrammetry, has been solved using new digital photogrammetry methods such as Structure from Motion (S*f*M). By using multiple overlapping images, S*f*M reconstructs the 3D scene structure, camera positions and orientations from a set of feature correspondences. The incorporation of bundle adjustment techniques, which consist of a non-linear refinement of camera and point parameters, has enabled to optimize S*f*M 3D reconstructions and to minimize reprojection errors. [28]. Many UAS are endowed with consumer-grade RGB cameras that provide excellent image quality in a relatively small and light package along with flexibility in imaging through their interchangeable lenses. As well, some RGB cameras have been created specifically for UAS applications.

Multi- and hyperspectral cameras are typically used for material identification and mapping purposes based on the study of the spectral signature of the different materials (vegetation, soils, water constituents, waste, etc.) rather than defining metric properties. These sensors sample multiple bands of the electromagnetic spectrum, from blue (400 nm) to near infrared (840 nm), short wave-length infrared (1800 nm) and mid-wavelength infrared (4000 nm). While multispectral cameras detect radiation in a small number of bands with relatively large bandwidth (20–40 nm), hyperspectral cameras can sample a broad range with a much higher spectral resolution, even higher than 200, with narrower bandwidths (2–5 nm). The reduced need for correction of the atmospheric effect thanks to the very low flight height of these platforms facilitates calibration using standards and field radiometry. Nevertheless, several environmental factors such as light angle, shades, water vapor content or technological constraints like the relatively high signal-to-noise ratio makes it necessary to apply certain corrections during image processing. Adao et al. [7] or He and Weng [29] among others, reviewed a range of hyperspectral sensors used with UASs.

TIR sensors are aimed at detecting long-wave infrared energy (8000–14,000 nm) emitted by objects in the camera's field of view. Since the emitted energy is directly proportional to the fourth power of the thermodynamic temperature of the surface, TIR sensors can be used to generate surface temperature maps but need to account for emissivity effects such as angle of observation or material. Another aspect to consider is the time of observation; while during day the recorded energy is a mixture of purely emitted and reflected radiation, in the absence of incoming radiation (e.g., during night) the energy and temperature maps show the truly emitted radiation of the surface. TIR sensors use microbolometers as detectors; devices that change their electrical resistance as a function of temperature.

This resistance change is measured and transformed into temperatures which can be used to create an image. Currently, there are two main types of commercial TIR systems; (i) sensors with cooled microbolometer arrays, which measure the short-medium wave IR, offer greater resolution and thermal sensitivity but are bulkier and more expensive and (ii) sensors with uncooled microbolometers, which work in the LWIR spectrum and are less susceptible to solar reflection. As cooled microbolometers are heavier, they are normally used in airplanes or satellites. Uncooled microbolometer on the other hand are lighter and cheaper, what makes them suitable to be mounted on UAS, but they can experience temperature drift issues [30]. This temperature drift problem is an inherent consequence of the set-up of the sensor; uncooled microbolometers are infrared sensors distributed in an array where each unit function as single sensor elements. Temperature drift in the system will occur due to temperature changes inside the camera or due to heating of the lenses or focal plane array. The most common approach to tackle with this issue is the application of non-uniformity corrections to remove noise, what leads to a more homogenized response signal along the microbolometer array [31,32]. In this regard, ref. [32] proposes a workflow for data acquisition and preprocessing along with best practices to reduce camera uncertainty in long and short-term noise. In recent years LiDAR (Light Detection and Ranging) sensors are being incorporated into lightweight UAS platforms. These sensor packages, which are active type, use lasers to scan the environment to produce 3D point clouds of the terrain, bottom of surface water bodies and vegetation.

Finally, in addition to the devices that remotely acquire information from objects avoiding any physical contact, UAS platforms can carry instruments such as multiparameter probes (temperature, electrical conductivity, pH, Eh, dissolved oxygen, oxidation-reduction potential, etc.) to be dipped into the water column, different types of samplers, Geiger counters or magnetometers or multi-gas monitors among others. In all cases, UAS constitute a platform from which conventional measurements can be carried out with great flexibility in terms of location and movement, reducing campaign costs and minimizing risks [33]. A general overview of the different types of sensors and their advantages, limitations and potential applications is provided in Table 3.

Table 3. Overview and some examples of sensors commonly used with UAS in hydrological research.

Types of Sensor	Spectral Ranges (nm)	Camera Examples from Cited Works	Hydrological Applications	Main Advantages and Disadvantages
RGB	~400–700	Canon Powershot G5/Canon EOS [34]	Visual analysis, bathymetry, DEM photogrammetry, water stages, flood monitoring, particle velocimetry, HAB [1] monitoring, mapping and classification of surfaces.	Advantages: (1) Wide range of prices, resolutions and weights available depending on the model. (2) Video capture. (3) Easy integration in different platforms.
		Zenmuse X3 FC350 [35]		Disadvantages: (1) Lower spectral resolution that makes them unsuitable for many tasks. (2) Very sensitive to environmental and ilumination conditions. (3) Some lack of geometric and radiometric calibration.
		RGB OLYMPUS EP-2 [36]		
		Nikon D500/D5100 [37]		
Multispectral	~400–1000	Rededge Micasense [38,39]	Bathymetry, HAB monitoring, river/lake trophic status, flood monitoring, SW–GW [2] interactions, wetland/river mapping, surface/material identification.	Advantages: (1) Wider range of applications compared to RGB sensors, allowing to discriminate/identify a variety of materials. (2) Some present means of radiometric calibration. (3) Allow geometric reconstruction. (4) Allow sub-decimetric mapping.
				Disadvantages: (1) Relatively high prices. (2) Detect radiation in a small number of broad wavelength bands, limiting their applications. (3) Currently, sensors are not optimised for aquatic applications. (4) Limited compatibility to UASs.

Table 3. *Cont.*

Types of Sensor	Spectral Ranges (nm)	Camera Examples from Cited Works	Hydrological Applications	Main Advantages and Disadvantages
Hyperspectral	~500–2500	Rikola 2D [36]	Bathymetry, HAB monitoring, river/lake trophic status, flood monitoring, water quality monitoring, wetland/river mapping, surface/material identification.	Advantages: (1) High spectral resolution data, with many narrow contiguous spectral bands that improve their ability to discriminate/identify materials.
		Nano Hyperspec [40]		Disadvantages: (1) High costs. (2) Size of sensors. (3) Need for spesialised software. (4) Low signal-to-noise ratio.
Thermal infrared	~8000–14,000	ThermoMAP [41]	River/lake temperature mapping, SW- GWD identification, thermal plumes identification, river discharge.	Advantages: (1) Validation is not required if only relativetemperatures are needed. (2) Relatively low cost. (3) Wide range of models and resolutions.
		DJI Zenmuse XT [42]		
		ICI Mirage 640 [43]		Disadvantages: (1) Temperature drift issues. (2) Radiation emitted from near-bank objects may impact the sensor, resulting in erroneous image interpretation. (3) Need for radiometric corrections. (4) TIR imagery interpretation can be complex and requires expertise. (5) Highly sensitive to <30° observation angles and changes in surface roughness.
		FLIR TAU2 640 [44]		
UAS LiDAR	~500–900	Phoenix Scout SL1 [45]	Bathymetry, 3-D mapping, water stages, flood monitoring.	Advantages: (1) Less susceptible to environmental conditions. (2) provides direct geometric measurements. (3) Possibility of discriminating the effect of vegetation.
		ASTRALiTE edge [43]		Disadvantages: (1) Limited by water clarity and bottom reflectivity. (2) High costs. (3) Few models compatible with UAS. (4) Need for groundfiltering corrections. (5) Strong dependence on accurate dynamic positioning systems.

[1] Harmful algal bloom; [2] surface water–groundwater.

4. UAS Applications in Surface Water Research

In the last two decades, UAS have become a widely applied tool in fluvial environments and specially in the study of river morphology. This has resulted in a large body of available literature reporting the use of UAS for the study of channel evolution and bedform migration, bank erosion, bed grain size and fluvial topography/bathymetry mapping among others [46–49]. Likewise, there is a growing number of papers addressing other hydrological aspects such as river stage fluctuations, water budgets, river discharge, surface velocity or flooding and temperature mapping. In addition to remote retrieval of data, in recent years, UAS are being used as platforms to deploy a variety of sensors, as water samplers or as key elements of water monitoring systems. This section presents a collection of studies focused on hydrological issues, the advances they represent and the role that UAS have played in their execution.

4.1. Bathymetry and Submerged Topography

Knowledge of river and stream bathymetry is fundamental to study fluvial processes and provides essential inputs to hydrodynamic models. Bathymetric measurements were traditionally carried out manually or using single/multibeam echo sounders mounted on vessels. These methods, which are not only time-consuming but also difficult to implement in deep streams and rivers with strong currents, have been progressively complemented with high resolution systems (remote sensing techniques, satellite imagery, aerial photography and laser scanning) and particularly, with UAS. In the context of remote

sensing, bathymetric mapping can be tackled with three approaches; (i) spectral methods based on the attenuation of the electromagnetic wave in the water column and the reflection from the bottom of the water body, (ii) photogrammetry, which uses sets of images recorded with imaging sensors to identify coordinates of points, boundaries and features in the images, and (iii) bathymetric LiDAR, which measures the time from pulse emission and echo reception, scattered back from the river/lake bottom within the instantaneous field of view. These remote sensing tools can significantly improve the accuracy and reliability of river geomorphology mapping and modeling specially when high topographical resolution is required.

Optical methods such as UAS photogrammetry were traditionally restricted to above-water studies, but nowadays their scope of application has been extended to below-water areas due to the development of refraction-correction algorithms. This has made possible to capture water surface and bottom features and water column characteristics as long as the system is not masked by vegetation or other obstacles and water is clear. One of earliest examples of this type of UAS application is provided by Lejot et al. [34], who launched a paramotor-paraglider equipped with a conventional RGB camera to acquire high resolution imagery and study channel water depth and gravel bar geometry at the Ain and Drome rivers (France). A simple empirical model that related radiometric signal with water depth was used to characterize aquatic zones of different size, yielding spatial resolutions of 5–7 cm. The water depth surveyed ranged from 0 to 5 m, and the results showed good accuracy until 3 m. The gravel bar was characterized through classical photogrammetry with a DEM generated using stereoscopic pairs, achieving 5 cm resolution. Although heterogeneous, the quality of both products was sufficient for bathymetric and channel microtopography mapping. In a pilot study Zinke and Flener [50] generated bathymetric maps at 2 sites of a gravel riverbed in Norway using drone-borne photography and the Lyzenga's deep water correction algorithm. Although the results of this study offered variable levels of accuracy and precision, the authors demonstrated the usefulness of UAS-based optical remote sensing methods to improve the effectiveness of bathymetric surveys. Flener et al. [37] created a seamless DEM of a subarctic river channel and plains combining mobile laser scanning and UAS-photography based bathymetric modeling. Albeit water depth in the study area did not exceed 1.5 m, the authors found quality issues in the UAS imagery that were mostly related to reflection (sunglint) and illumination changes during the flight. Accuracy varied depending on the combination of methods applied. Despite these problems, the UAS-photography-bathymetric model gave depth accuracies below 10 cm, which is suitable for applications such as hydraulic modeling or habitat studies, but insufficient for more detailed studies.

On the other hand, structure from motion (S*f*M), has been widely used in fluvial bathymetry in recent years. For instance, Woodget et al. [51] quantified the exposed and submerged topography of two river reaches (depths ranging from 0.14 to 0.70 m) in UK through S*f*M photogrammetry. An UAS equipped with a RGB consumer-grade camera was used to produce DEMs with hyperspatial resolutions of 2–15 cm. Mean errors in submerged areas ranged between 1.6–8.9 cm but were significantly reduced after the application of a simple refraction correction, reaching values between −2.9 to 5.3 cm. Dietrich [52] retrieved fluvial bathymetric measurements from UAS imagery and S*f*M and proposed a multicamera-based refraction correction method for off-nadir S*f*M datasets. In this case, the surveyed water depth varied between 0 and 1.5m. The bathymetric datasets obtained after the correction showed precisions of ~0.1% of the flying altitude (40 and 60 m above ground level), which makes this method suitable for a range of fluvial applications. Entwistle and Heritage [53] generated a S*f*M-derived DEM with imagery collected from a small UAS to predict water depth and map bathymetric surfaces. The results from the S*f*M survey were compared with others from a theodolite survey, showing similar accuracy and precision (0.85 R^2 value after using a 1.02 multiplier on the regression line up to depths of 1 m), thus demonstrating that the UAS approach proposed could achieve good depth estimations. Carrivick and Smith [16] reviewed the applications of S*f*M photogrammetry and UAS

technology in aquatic environments, highlighting the need of automated procedures to correct refraction. The issue of refraction correction has been addressed in several works; Woodget et al. [35] quantified above and below-water geomorphic changes in a river through S*f*M photogrammetry and analyzed the implications of refraction, water surface elevation and the spatial variability of topographic errors. They demonstrated that it is possible to quantify submerged geomorphic changes with levels of accuracy of less than 4 cm similar to that from exposed areas without the need of calibration data and that, using nadir imagery, the results obtained after different refraction corrections are practically the same. Partama et al. [54] presented a novel technique based on co-registered image sequences or video frames to reduce the effects of water-surface reflection on UAS-based photogrammetry. This promising method, applied in a river reach 0–1.5 m deep, achieved accuracies of 5–15 cm, clarified the reflected signal from the bottom bed and enabled to reduce moving light patterns. The issue of refraction correction has been addressed by several authors, although most works focus on the marine environment, for instance Skarlatos and Agrafiotis [55] proposed an iterative algorithm that, applied at the photo level, could reduce the effect of refraction to 2 times the ground pixel size within the photogrammetric workflow. Also in marine environments, Agrafiotis et al. [56,57] provided a deep-learning framework to automatically correct water refraction errors. The method consisted in a support vector regression model based on known depth observations from bathymetric LiDAR surveys, which enabled to estimate the real depth of point clouds obtained from S*f*M and multi-view-stereo techniques. The model demonstrated great potential in terms of depth accuracy in shallow waters and can be used when no LiDAR data are available.

River depth estimations have also been successfully retrieved from UAS hyperspectral data; Gentile et al. [36] used very high spatial resolution hyperspectral images and an empirical model to map the bathymetry of a shallow river, achieving a good fit in the spectral range from 700–800 nm and average errors of even less than 13 cm at depths between 9–101 cm.

On the other hand, LiDAR sensors were rarely implemented in UAS owing to their high costs and usually excessive weight, however, these issues are being overcome leading to the democratization of these systems and making their use increasingly frequent. For these reasons, until recently, a widely applied alternative to optimize photogrammetric DEMs and produce more accurate products was the complementary use of satellite, airborne or land-based LiDAR data and UAS optical images. The performance of multispectral satellite imagery, hyperspectral data from manned aircraft and UAS, and water penetrating green LiDAR to map fluvial bathymetry was assessed by [40] in a short reach of Sacramento River with a mean depth of 1.8 m. LiDAR systems offered greater accuracies, while UAS-borne products tended to underpredict depths, reaching R^2 values of 0.95 and 0.88 respectively. However, the maximum detectable depth for the LiDAR sensor was an important constraint due to the lack of bottom returns at depths greater than 2 m. Given the constraints of remote sensing of river bathymetry, the authors advocate for a hybrid field and airborne approach but recommend the use of hyperspectral or multispectral UAS imagery for small channels and fine-scale information owing to their versatility, high spatial resolution and the possibility of collecting targeted and task-specific data. A major leap forward for river mapping is the methodology presented Mandlburger et al. [58] who developed a novel compact topo-bathymetric laser scanner designed for integration on UASs and other types of aircrafts. The sensor comprised an IR laser that emitted pulses at a wavelength of 532 nm with a duration about 1.5 ns pulse and a pulse repetition rate of 50–200 kHz. The laser had a 10–30 cm footprint on the ground and yielded a point density of 20–50 points/m^2, which made it particularly well suited for capturing river bathymetry. The system was tested in freshwater ponds with an overall depth of 5–6 m and turbid bottoms. Although the system presented a maximum vertical deviation of 7.8 cm and a systematic depth-dependent error, the sensor showed great potential for hydrology and

fluvial morphology applications owing to its good depth performance, accuracy and high spatial resolution.

Bathymetric analysis has also been addressed with multiplatform and multisensor approaches. Kasvi et al. [59] addressed the accuracy of shallow water (0–1.5 m) bathymetric mapping through the implementation of three remote sensing techniques: optical and bathymetric S*f*M modeling, both from UAS data, and a remote controlled acoustic doppler current profiler (ADCP) coupled with an echo-sounder. Their results (Figure 3) emphasized how the characteristics of the study site such as river size, depth and water quality determine the results and suitability of each method.

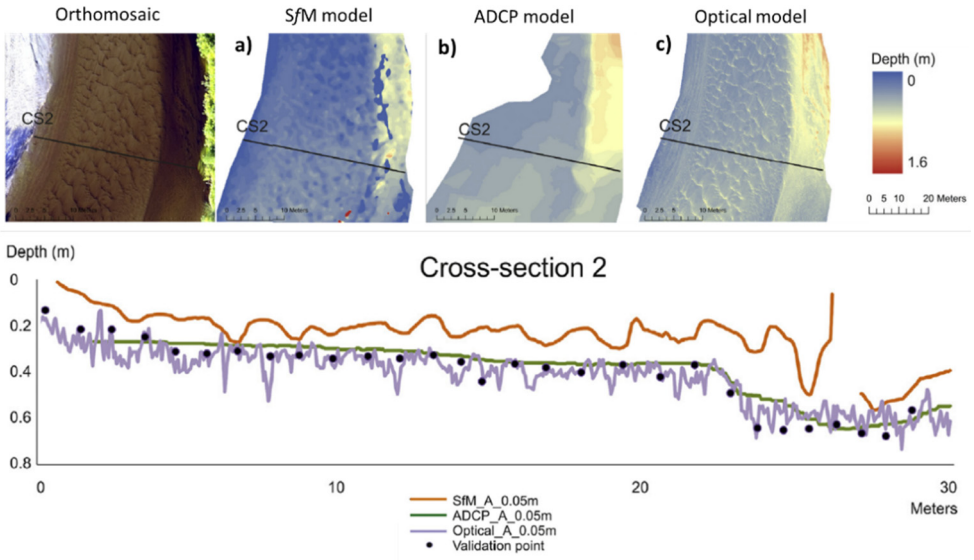

Figure 3. Orthomosaic and bathymetric models of 5 cm resolution obtained from (**a**) structure from motion (SfM), (**b**) acoustic doppler profiler and (**c**) optical modeling. CS2: cross-section of the river studied. Modified from [59].

Although the results of the echo-sounding were less detailed and restricted to depths over 0.2 m, they were the most accurate. On the other hand, the bathymetric S*f*M was highly sensitive to flow turbidity, color and therefore depth, with mean errors that increased notably at depths >0.8 m and notably changed between autumn (−50 cm mean error) to spring (−120 cm). Optical modeling, was very sensitive to substrate variability, color and depth. This evidences that bathymetric S*f*M is more suitable for clear waters and structured and visible riverbeds. Erena et al. [60] proposed a method to create updated capacity curves for 21 reservoirs of the Segura River Basin (Spain). Their study integrated bathymetric measurements acquired using an Unmanned Surface Vehicle (USV) and an Unmanned Underwater Vehicle (UUV) with a DSM generated from UAS imagery and airborne LiDAR data. Apart from evidencing a substantial silting in the reservoirs, this multiplatform methodology demonstrated being more efficient than the traditional methods.

UAS have also been used to deploy bathymetric measurement instruments such as sonars. This is the case of the study by Bandini et al. [61], who measured accurate water depths in lakes and rivers of Denmark using a tethered floating sonar controlled by an UAS. This method, which enables to monitor dangerous or inaccessible areas, yielded significantly accurate results (~2.1%) although some observational bias (attributed to the dependence of the sound wave speed on temperature, salinity, and pressure) was detected. In a U.S. reservoir, Álvarez et al. [62] implemented a novel bathymetric survey method by merging two UAS-based sampling techniques; (i) a small UAS that propelled a mini boat equipped with a single-beam echosounder for surveying submerged topography in deeper waters and (ii) S*f*M photogrammetry to cover shallower areas visible from the UAS but not detected by the echosounder. The UAS-S*f*M data successfully complemented the echosounder survey and minimum depths from 0 to 5 cm were detected.

Finally, it should be noted that many studies on bathymetric reconstruction of shallow streams and reservoirs proved that models derived from high resolution UAS data are more robust than previous models based on conventional methods, reducing inaccuracies and biases, and enabling better hydraulic modeling performance [63–66].

4.2. Water Level Measurement and Water Storage

Albeit the temporal and spatial fluctuations of water stored in rivers, lakes, reservoirs and wetlands are among the most important hydrologic observations, the current knowledge of these variables is still considerably improvable, limiting our water management and forecasting capacity. Water level measurements have been traditionally made with limnimetric scales and limnigraphs, which despite being useful for determining water stages, only provide information of very specific points in the water body. The translation of water levels into stored volumes can be complicated and give imprecise results. In this regard, achieving a better understanding of these processes and reliable hydrologic predictions require accurate observations of several variables, such as surface water area, water level elevation, slope and temporal changes [67]. In this context, UAS are playing a key role in quantitatively characterizing and monitoring water level and their usefulness has been demonstrated in recent works. For instance, UAS allow to retrieve data from inaccessible environments and to overcome the disadvantages of traditional static sensors, which can be deployed in limited numbers and imply higher personnel and maintenance costs. UAS imagery has been used to obtain rapid observations of water level fluctuations in large-scale hydrological systems such as reservoirs. Ridolfi and Manciola [68] proposed a sensing platform that allowed to measure the water level and collect hydraulic information during adverse operation conditions such as floods. Water level in a dam was retrieved from the combination of UAS-based RGB imagery and optical methods based on ground control points and edge detectors. Their results were promising and proved the suitability of the platform for hydraulic measurement acquisition, however, the pixelization of the images and the perspective constituted an important source of uncertainty. Gao et al. [69] devised an innovative methodology that integrated UAS photogrammetry and image recognition to define water level in a complex hydrological environment (plunge pool downstream a hydropower station) in China. Water surface fluctuations were captured by an UAS and the regions of interest were extracted from imagery. The relationship between image pixel scale and actual spatial scale, the real water surface elevation and fluctuations, as well as the maximum, average and minimum water levels were obtained applying specific calibration coefficients. The method was successfully implemented and offered reliable results that back its potential to monitor water level.

The water level in rivers and lakes was estimated in [70] using three types of sensors (radar, sonar and a camera-based laser distance sensor) capable of measuring the range to water surface onboard lightweight UAS. Water surface level was calculated by subtracting the range measured by the sensors from the vertical position retrieved by the onboard GNSS receiver. The radar offered the best results in terms of accuracy (0.5% of the range) and longest maximum range (60 m), whereas the sonar was more appropriate for stable and low flight altitude. The laser system gave less accurate results but proved to be useful for narrow fields of view. This system proved that water level measurements acquired with ranging sensors and GNSS receivers can provide more accuracy than spaceborne or airborne altimetry. In a more recent work, ref. [71] retrieved water surface elevation (WSE) measurements in very small vegetated streams (1–2 m wide) using a drone-based radar altimetry solution with full waveform analysis. The water surface elevations measurements provided by this system were one order of magnitude better than those obtained from LiDAR or photogrammetry. Following a similar approach, Jiang et al. [72] deployed a UAS-based radar altimetry system to map spatially distributed WSE in a small vegetated stream and subsequently used the dataset obtained to calibrate and validate roughness parameters in hydrodynamic models. UAS altimetry delivered WSE observations with 3 cm accuracy and 0.5 m resolution and could identify significant variations of the Manning–Strickler

coefficients over time. The study demonstrated that UAS-borne WSE constitutes a useful tool to understand the variations of hydraulic roughness. In order to assess the usefulness of various UAS geospatial products in water body recognition, Tymkow et al. [73] combined data from UAS-based laser scanner, thermal infrared and RGB imagery to estimate the water extent of several rivers and lakes. According to their results, the most suitable product in water body detection was four bands RGB + TIR (Thermal InfraRed) orthomosaic, achieving an average kappa coefficient above 0.9.

On the other hand, S*f*M is currently offering promising results in the reconstruction of free water surfaces. The potential innovative applications of this technique have been highlighted in several recent works. Niedzielski et al. [74] observed the water stages in the Scinawka river (SW Poland) by combining UAS RGB imagery and S*f*M algorithms to generate multitemporal orthophotomaps without using ground control points. The authors detected statistically significant increments in water surface areas between orthophotomaps using asymptotic and bootstrapped versions of the Student's t-test. This approach proved to be effective in detecting statistically significant transitions produced by all characteristic water levels, from low and mean, to high stages, and can be used to verify hydrodynamic models, monitor the water level in ungauged basins and predict high flows. A methodology to estimate the water storage in seasonal ponds is provided by García-López et al. [75] (Figure 4). The authors defined the geometry of a coastal wetland's basin in pre-flood conditions via UAS photogrammetry and S*f*M techniques. The DEM generated allowed a spatial resolution of 6.9 cm and a mean squared error in Z of 5.9 cm with a practically nil bias and resulted an order of magnitude better than the pre-existing official LiDAR cartographic products. Although the effect of vegetation on the DEM was the main obstacle to the application of this method and it had to be minimized through spectral and morphological techniques, as a whole, this approach proved to be useful for calculating the water balance in this type of systems.

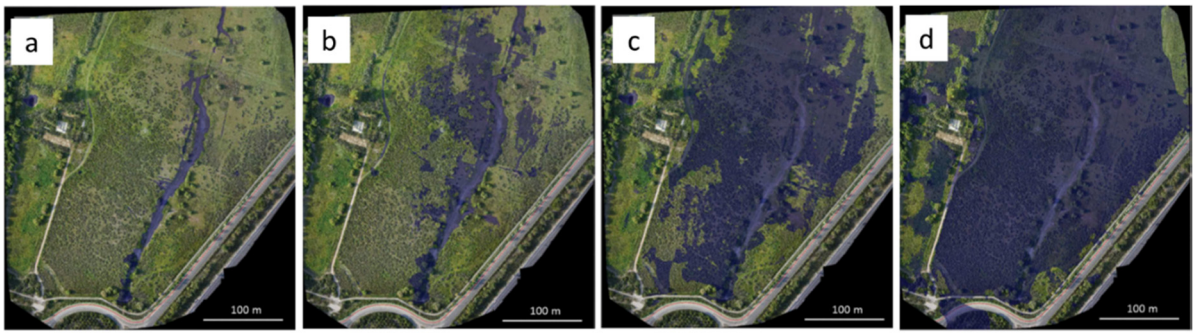

Figure 4. Prediction of the flooded area according to different water levels ((**a**) 1.80, (**b**) 1.90, (**c**) 2.00 and (**d**) 2.20 m with respect to the mean sea level) from UAS-derived DEM. Modified from [75].

To identify the river stages along the Kilim river (Malaysia), Mohamad et al. [76] generated DSM and orthomosaics for different tidal phases through the combination of UAS-based photogrammetry, GNSS vertical data and the use of the S*f*M algorithm. Although the study achieved a limited vertical precision, it may be useful for future works on water level measurement in estuaries and systems influenced by tides. S*f*M techniques have also been employed in the mining field by Yucel et al. [77] to analyze the areal changes and evolution of lakes originated by acid mine drainage. More recently, Chen et al. [45] developed a ground-filtering method to remove the effect of vegetation in wetland´s water budget estimations, thus improving the DEM obtained from UAS photogrammetry. Their approach comprised the combination of airborne LiDAR products with UAS LiDAR, UAS photogrammetric surveys and the application of a linear-weighted-average filter to generate a filtered DEM where the vegetation interference in the bathymetric data was reduced. The ground-filtered DEM showed a 90% correlation with in situ measurements, diminished the errors in water balance and reduced the uncertainties in the results.

4.3. Surface Velocity and Flow Estimations

Runoff and river discharge constitute a fundamental element of the water balance and is of critical importance for the sustainable management of water resources, freshwater ecosystems integrity and flood forecasting, among others. Although river discharge is one of the most accurately measured components of the hydrological cycle, the access to this information remains limited. The reasons are that large extensions of river basins around the globe are still poorly gauged or even ungauged [78], the decline in hydrometric stations, the gaps in datasets, the need for improved methods for the storage, retrieval and processing of hydrometric information [79].

Traditionally, discharge measurements have been carried out through direct and indirect methods. The first consist of the definition of the river section and flow velocity with mechanical current-meters, ADCP, tracers, etc. Indirect methods are based on the measurement of water surface level at gauging stations, which provide flow estimations through rating curves. Remote sensing and satellite altimetry on the other hand, has been widely used to successfully calculate river discharge in well-known large rivers of the world [80,81]. However, this methodology is less suitable for medium/small rivers and presents limitations related to the measurement of the average flow velocity and slope, the need of calibration with in situ measurements, poor spatial and temporal resolution and other issues. In this line, UAS have been increasingly used in the estimation of river discharge and flow as they overcome the handicaps of satellite remote sensing and present some advantages over it in terms of data accuracy.

Some authors propose the combined use of UAS with traditional hydrological formulas to calculate river discharge in ungauged areas. Yang et al. [82] calculated the river discharge in ten sections in the Tibetan Plateau and Province of Xinjiang by (i) retrieving the parameters of the slope-area method using an UAS to generate a digital orthophoto map and a DSM and (ii) applying three different formulas (Manning–Strickler, Saint-Venant and Darcy–Weisbach). In Yang et al. [83], UAS remote sensing, high altitude remote sensing and in situ measurements are combined to estimate river flow in medium/small wide shallow rivers in arid areas. The attenuation coefficient and discharge of the ungauged Hotan river (Central Asia) was calculated by applying energy equations and a trapezoidal cross-section discharge equation. Similarly, UAS-borne data were used to verify the river section morphology through orthophotomaps and a DSM, reaching a centimeter level accuracy. Both studies proved the usefulness of UAS for carrying out rapid river discharge assessments and provide relevant hydrological data in poorly gauged or ungauged systems. Lou et al. [84] integrated UAS and satellite remote sensing (Gaofen-2, SPOT-5, and Sentinel-2) with the application of hydrological formulas (Manning–Strickler) to obtain accurate discharge values from 24 ungauged rivers in the Tibetan Plateau on a long term scale, extending the previously mentioned works.

In addition, the monitoring of surface velocity has been addressed through UAS-based videos and the application of particle tracking velocimetry methods using natural and artificial tracers. Koutalakis et al. [85] compared the results obtained from the analysis of UAS imagery with 3 specific software based on different velocimetry methods: large-scale particle image velocimetry (LSPIV), large scale particle tracking velocimetry (LSPTV) and space-time image velocimetry (STIV). Although the three methods displayed similar trends, the surface velocity values differed slightly in some vegetated parts of the river reach and the authors point out the need for verification. Similarly, ref. [86] used UAS-borne imagery to evaluate the sensitivity of 5 image velocimetry algorithms under low flow conditions and concluded that, for surface velocities of approximately 0.12 m/s, image velocimetry techniques can provide results comparable to traditional techniques such as ADCPs. Tauro et al. [87] presented a custom-built UAS platform equipped with a ground-facing orthogonal camera that did not require image orthorectification, to monitor the surface flow through LSPIV in a natural stream. This low-cost system expands the use of traditional fixed cameras employed in particle velocimetry by enabling access to otherwise inaccessible areas. Tauro et al. [88] assessed the suitability of a low cost UAS

for creating accurate surface flow maps of small-scale streams. After calibration, flow velocity maps were extracted from the motion of stream floaters at real-time by applying the LSPIV high-speed cross-correlation algorithm. Similarly, ref. [89] integrated LSPIV and UAS imagery and compared the discharge values obtained with that from other methods, such as a fixed camera, ADCP, stream gauges and a propeller meter. The authors also report the minimum steps required to produce accurate LSPIV measurements using UAS.

Despite its many advantages, the accuracy of the image velocimetry method is conditioned by several factors such as seeding density, the environmental and experimental setting conditions or the presence of floating materials on the stream surface. In this regard, ref. [90] used high-definition UAS footage to test the precision of LSPIV and particle tracking velocimetry methods under different seeding and hydrological conditions. The authors demonstrated that seeding density, dispersion index and the spatial variance of tracer dimension are statistically relevant metrics in the estimation of velocity and that a prior knowledge of seeding conditions can be useful for selecting the processing intervals, image velocimetry techniques to apply and for controlling the accuracy of results.

Time series of temperature images have also been used for estimating surface flow velocities. Kinzel and Legeiter [43] proposed a methodology to estimate river discharge through the combination of thermal velocimetry and scanning polarizing LiDAR, both UAS-based. The velocity of surface features, expressed as small differences in temperature, was tracked with a particle image velocimetry algorithm. The system was able to detect the movement of flow features expressed as subtle differences in temperature, with velocity measurements that agreed closely with that made in situ. However, depths inferred from the LiDAR showed less agreement with in situ measurements in the deeper sections of the river. Another innovative approach was proposed by Thumser et al. [91] who measured real-time river velocity using floating, infrared light-emitting particles and a color vision sensor onboard a UAS to track the position of objects. The system, termed by the authors as RAPTOR-UAV, enabled to capture large-scale, nonstationary regions of the velocity field where the flow fields are persistent and chaotic. Recently, remote sensing of surface velocity and river discharge has been addressed in [92] through UAS-based doppler radars yielding results comparable to conventional streamgaging if cross-sectional area is available.

4.4. Flood Monitoring

Floods are among the most important driving forces in fluvial environments. These periodic events not only reshape floodplain landscape and riverbeds, but also contribute to basin connectivity facilitating the exchange of water, sediments, organic matter, and nutrients between rivers, floodplains, and riparian wetlands. However, floods can also have dramatic impacts on human societies, causing economic damage, health issues, and loss of human life, infrastructures and productive land. For this reason, gathering information on flooding conditions and dynamics and determining the extent of floods at different scales is crucial for predicting and mitigating the impact of this natural hazard. Over several decades, flood hazard assessment and inundation mapping has been addressed through the use of satellite remote sensing. Nowadays, UAS provide very high-resolution imagery on-demand and are being increasingly used in geohazard studies and monitoring.

UAS-based photography has been extensively used to acquire data in inaccessible locations and create high resolution DEMs, map flood-prone areas and to enhance hydraulic modeling [93–97]. In particular, S*f*M techniques have seen a strong development as an alternative approach to classical digital photogrammetry in the study of floods, leading to an increasing body of literature in the last years; Özcan and Özcan [98] extracted a high-resolution DEM of a flood-vulnerable river in Turkey applying UAS-based SfM. Landform alterations due to erosion and deposition after flood events were analyzed through the application of DEM of difference algorithm (DoD) and geomorphic change detection (GCD) techniques. After a 2-year monitoring period, the authors verified that UAS S*f*M and DoD were useful tools for geomorphological dynamic mapping and flood event monitoring. Diakakis et al. [99] investigated one of the most devastating floods occurred

in Greece in 40 years through the combination of systematic ground measurements and UAS observations during and after the event. Highly detailed DSM with 2.7 cm resolution derived from S*f*M were used to obtain the flood extent, depth maps and the peak discharge, as well as a comprehensive description of the physical characteristics of floodwaters across the inundated area (Figure 5). An analysis of the flood impacts on geomorphology, vegetation, infrastructures and human population was also carried out.

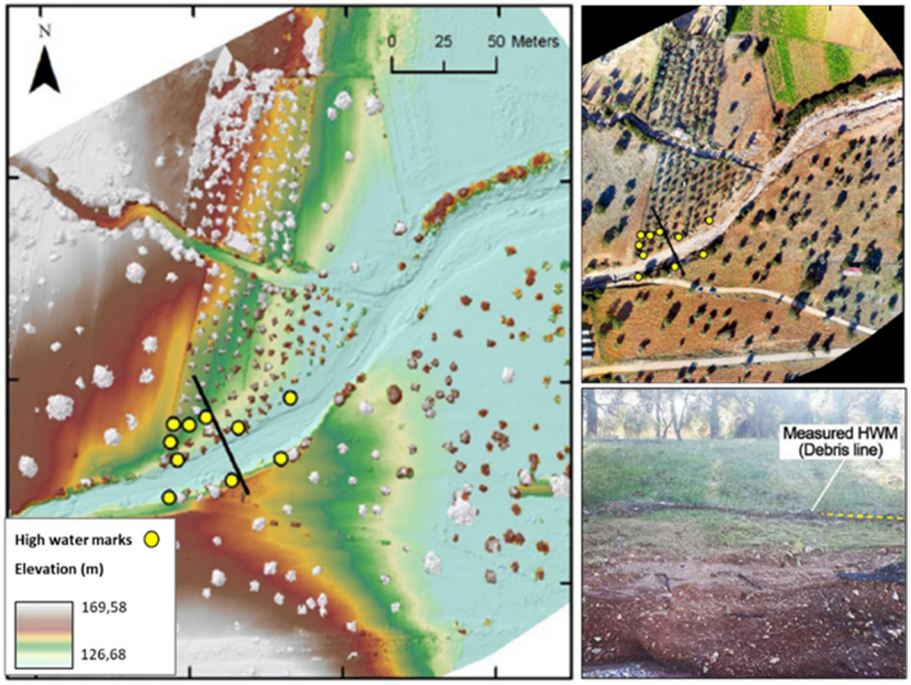

Figure 5. Digital surface models (DSM) derived from SfM and high-water marks identified upstream and downstream a cross section (indicated by a black line) of the river after a flood event. Modified from [99]. Copyright 2021 Elsevier.

Moreover, UAS S*f*M photogrammetry is being increasingly applied to flood research as an alternative to LiDAR techniques owing to its more flexible image acquisition, the lower costs and the availability of powerful processing tools that generate DEM and DSMs in a single workflow. As several authors have pointed out, the recent advances of UAS-S*f*M provide accuracies comparable to that obtained by LiDAR. For instance, Leitão et al. [100] evaluated the suitability of several UAS-derived DEMs (obtained with different flight parameters) for urban overland flow and flood modeling in Switzerland and compared them with an aerial LiDAR DEM from the Federal Office of Topography (SwissTopo LiDAR). According to their results, the quality of both products were comparable and differences were not substantial, especially in building, vegetation and tree free areas. For instance, the minimum, maximum, mean, and standard deviation of the elevation differences between the UAS and LiDAR DEM was −0.468, 0.306, 0.06, and 0.119 m respectively, and differences in slope were always below 10%. However, the UAS DEM suffered from a major limitation; it did not cover the whole area of interest (e.g., areas behind buildings). Hashemi-Beni et al. [101] assessed the quality of UAS-derived DEMs for mapping a flood event and its extent during a hurricane in North Carolina (USA). The water surface extracted from the UAS-derived DEM was compared with LiDAR and stage gage data, demonstrating general agreement between models. More recently, ref. [102] used a fixed-wing UAS equipped with a conventional RGB camera to generate very high resolution bare-earth DEMs of a small river floodplain in Maryland, USA. The accuracy of the model was compared with the pre-exiting LiDAR models, obtaining a trivial bias of 1.6 cm and a root mean square derivation of 39 cm, which demonstrate the suitability of this method. Annis et al. [103] compared the suitability of UAS-derived DEMs, freely available

large-scale DEM and LiDAR DEMs for flood modeling in small basins. The authors proved that DEMs generated from UAS imagery significantly outperformed the large-scale DEM, and that drone-derived topography constitutes an appropriate alternative to LiDAR DEMs.

Another recent development in DEM generation methods is the combination of S*f*M and multi-view stereo (MVS) 3D reconstruction techniques. In a typical S*f*M-based process, the application of MVS algorithms follows image matching and allows to generate dense 3D point clouds from large sets of images. Villanueva et al. [104] assessed the DEM accuracy achieved from a S*f*M-MVS processing chain using LiDAR-derived control points and compared the estimations of flood volume and area obtained from UAS and LiDAR data. The authors concluded that UAS based DEMs were as accurate as LiDAR DEMs.

Reconstruction of flood episodes is also crucial to better evaluate and prevent potential risks in the future, being thus necessary precise information on flood extents, flow peaks, depths as well as on factors that might worsen the outcomes of the event. High resolution pre- and post-flood topographic data and UAS-derived ortho-imagery (4–5 cm/pixel) were employed by [105] to analyze three-dimensional morphodynamic changes associated with an extreme flood event in the Elbow River (Canada). Subsequently, geomorphic changes were assessed using the DEMs and their relationship with flow conditions were analyzed with a 2D hydrodynamic model. The authors documented large elevation changes, widespread bank erosion and channel widening after the flood and highlighted potential relationships between flood forces and geomorphic change. Abdelkader et al. [106] employed an UAS as a platform for Lagrangian flood sensing. The aircraft dropped small disposable buoyant wireless sensors that were carried away by the flood and transmitted real-time data that were used to map the extent of the inundated area. This method enabled accurate estimations of local flood parameters and short-term forecast of flood propagation.

Computer vision techniques and machine learning have also been used to classify remotely sensed imagery of flood events, e.g., [107] proposed a novel method for the detection and segmentation of flooded areas based on texture and color analysis in a deep neural network. The system, supported by ground control stations and a fixed wing UAS for image acquisition, increased the accuracy of flooded area detection up to 99.12%. Gebrehiwot et al. [108] applied a deep learning approach based on convolutional neural networks (CNN) to extract the flooded areas from UAS-borne (fixed wing and multicopter) RGB imagery. This method, implemented immediately after two hurricane events over 3 flood-prone areas in the USA, yielded a highly accurate classification (97.5%) of the remotely sensed data. Jakovljevic et al. [109] generated flood risk maps from LiDAR and UAS-derived data through a novel methodology based on raw point cloud classification and ground point filtering using neural networks. Flood risk assessment was calculated at 12 different vertical water levels. Although the UAS-derived model was less accurate than LiDAR and tended to overestimate the elevation, the overall approach met the accuracy required for flood mapping according to European Flood Directive standards.

In addition to the aforementioned applications, UASs constitute the most efficient and fastest tool for situational awareness in disaster management, not only providing accurate and spatially detailed hydrologic information during flooding events, but also enabling to identify safe shelter points, detect stranded people and damaged properties and to define future action strategies [110,111].

Nevertheless, although UASs have demonstrated to be a very useful tool in flood monitoring and delineation, they cannot substitute ground-truth measurements in this field since they cannot provide data on flood depth and the quality of the topographic products is compromised when the terrain is masked by vegetation or anthropogenic features. This issue has been recently addressed by [112], who reconstructed the flash flood events of two ungauged ephemeral streams in Olympiada region (North Greece) through the combination of ground-based and UAS observations and hydraulic (HEC-RAS) with hydrological (SCS-CN) models. Although the comparison between the modeled and observed flow extents showed a good performance of the hydraulic model, the modeled

flood depths displayed an overestimation attributable to the low resolution and quality of the DEM especially in the urbanized and vegetated areas of the floodplain.

4.5. Temperature Mapping

Temperature is one of the most important variables that control the chemical and biological processes within water bodies and determine the spatio-temporal distribution of habitat niches for many aquatic species. TIR remote sensing not only enables to detect groundwater discharge into inland and coastal systems, an aspect that will be discussed in Section 5, but also allows to measure longitudinal and transversal temperature heterogeneities in rivers, to study their temporal variability and to identify aquatic thermal refuges among other features.

UASs have emerged as alternative tools to traditional high-resolution TIR remote sensing or ground-based thermography, allowing to collect data at a spatial scale intermediate to both approaches and to conduct multiple surveys in a brief period of time. However, as TIR river mapping is based on the quantification of temperature from the amount of energy emitted by a water body, the quality of the measurements can be impacted by diffuse reflections from solar radiation if surveys are not conducted during the night or by factors such as surface roughness (e.g., riffles) that might alter the energy received by the sensor. Emissivity on the other hand can be altered by suspended sediment and dissolved minerals. Other sources of uncertainty are shadows cast by riverbank objects or the presence of foam, which can be misleading in the detection of discrete features such as cool water patches. In addition, the angle of observation is of the utmost importance. At oblique viewing angles above 30° water's emissivity is reduced as a function of increased specular reflection [113]. These problems can be ameliorated by careful selection of flight parameters (flight time, flight altitude and angle of observation) and type of sensors, and by supporting thermal with simultaneous optical imagery.

Early attempts of thermal image acquisition consisted of handheld TIR cameras adapted to be mounted on UASs [114,115]. Jensen et al. [114] combined a low-cost UAS-based visible, NIR and TIR imagery to generate surface temperature maps with 30 cm resolutions in order to identify the thermal patterns of a highly dynamic stream in northern Utah (USA). On the other hand, the thermal patterns of braided rivers in the French Alps are analyzed in [115] using an UAS equipped with an RGB and a TIR camera. In this case, a powered paraglider was employed to acquire the TIR images, which allowed to predict habitat diversity from temperature heterogeneity. More recently, Collas et al. [41] obtained UAS-borne high resolution imagery of a river side channel using a consumer-grade TIR camera to map sub-daily temperature heterogeneity and habitat suitability for native and alien fish species. The authors achieved an accuracy in water temperature estimates of 0.53° over all flights, thus demonstrating the usefulness of UASs TIR imagery for temperature mapping and habitat management. Dugdale et al. [42] assessed the results of UAS-based TIR surveys applied to the study of diffuse temperature and discrete thermal inputs (springs, culverts, tributaries) in rivers of USA and Scotland. The data obtained were strongly biased, which the authors attributed to sun glint (linked to flight characteristics), the impact of radiative warming on the camera and to internal heating of the sensor. This generated substantial differences between radiant and kinetic temperatures in the rivers studied, making it necessary to apply substantial corrections. Temperature drift, inherent to uncooled microbolometers, can be compensated through hardware and software solutions. This issue has been recently addressed by several authors such as Mesas-Carrascosa et al. [31] who provide an overview on the topic and present a correction methodology based on redundant information from multiple overlapping images, or Kelly et al. [116] who propose a set of best practices to minimize temperature drift of TIR cameras.

Another limitation is that TIR sensors can only measure the skin temperature of water bodies. This issue, however, has been recently overcome through temperature sensor-integrated-UASs, which enable the mapping of the thermal structure of shallow water

bodies. Chung et al. [117] developed an UAS equipped with a temperature probe that was dipped into the water to record temperature throughout the water column. Albeit the temperatures measured from the UAS were higher than those obtained in situ even after calibration, this system have the potential to enable high resolution 3D temperature mapping if some minor improvements are applied. Similarly, Koparan et al. [118] designed an UAS-based temperature profiling system that measured water temperature and depth. A key factor in their study is that the UAS system could land on and take off from water surface, avoiding hoovering during the measurements, reducing battery use and enabling more precise depth measurements.

To geolocate thermal plumes and collect temperature depth profiles over relatively larger scales (100 m to kms), DeMario et al. [119] integrated an IR camera and an immersible temperature probe in an UAS (Figure 6). This approach is especially useful for monitoring thermal effluents from power plants and can potentially displace the current boat-based operations usually implemented to characterize such discharges.

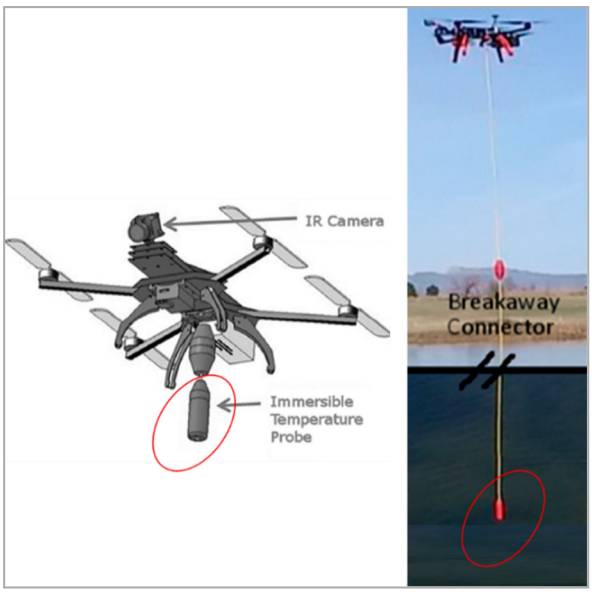

Figure 6. UAS platform designed by De Mario et al. (2017), equipped with an infrared (IR) camera for mapping water surface and a temperature probe to record the temperature depth profile. Modified from De Mario et al. [119].

Other applications of UAS include the monitoring and assessment of the effects of stormwater on the temperature of urban streams. Caldwell et al. [120] characterized the temperature response of a large urban stream in Syracuse (NY) to stormwater inputs by combining UASs-based TIR imagery with in situ sensors and pairing the observations with a deterministic stream temperature model. The authors quantified and characterized the creek´s temperature heterogeneities and the relative magnitude and extent of stormwater plumes. The study demonstrated the utility of airborne TIR imagery for simulating hydrologic processes, heat exchange and for revealing complex interactions between urban effluents and stream water temperature.

4.6. Water Contamination

Pollution of freshwater bodies is a ubiquitous problem that has drawn the attention of the scientific community, water managers and policy makers for a long time due to the serious public health and environmental risks that it poses. The pollutants that reach rivers, lakes and wetlands are extremely varied in nature, composition and source, being closely linked to anthropogenic activities and land use. The effective management of these substances and the prevention of their potentially harmful effects require the understanding and prediction of their transport, dispersion and behavior within the aquatic systems.

4.6.1. Dispersion Processes

UAS technology is enabling the rapid filling of knowledge gaps in the transport of pollutants and other hazardous agents while overcoming the difficulties inherent to in situ measurements. Powers et al. [121] coordinately used an UAS and an USV to detect and track dye released in a reservoir. The UAS was used to capture videos and images of the dye plume and to provide visual navigation of the tracer for the pilot of the USV. The dye concentration measurements collected by the USV were compared with that from UAS imagery, yielding similar results and demonstrating that processed images from UAS can be used to predict dye concentrations near the water surface. Baek et al. [122] estimated the concentration of fluorescent dye in an open channel using UAS RGB imagery. The authors applied an artificial neural network (ANN) to establish the empirical relationships between the digital numbers in the images and the spatio-temporal distribution of dye concentration (Figure 7). Although the ANN models required simultaneous in situ measurements, the authors demonstrated the feasibility of generating accurate high-resolution dye concentration maps with this novel and cost-effective approach.

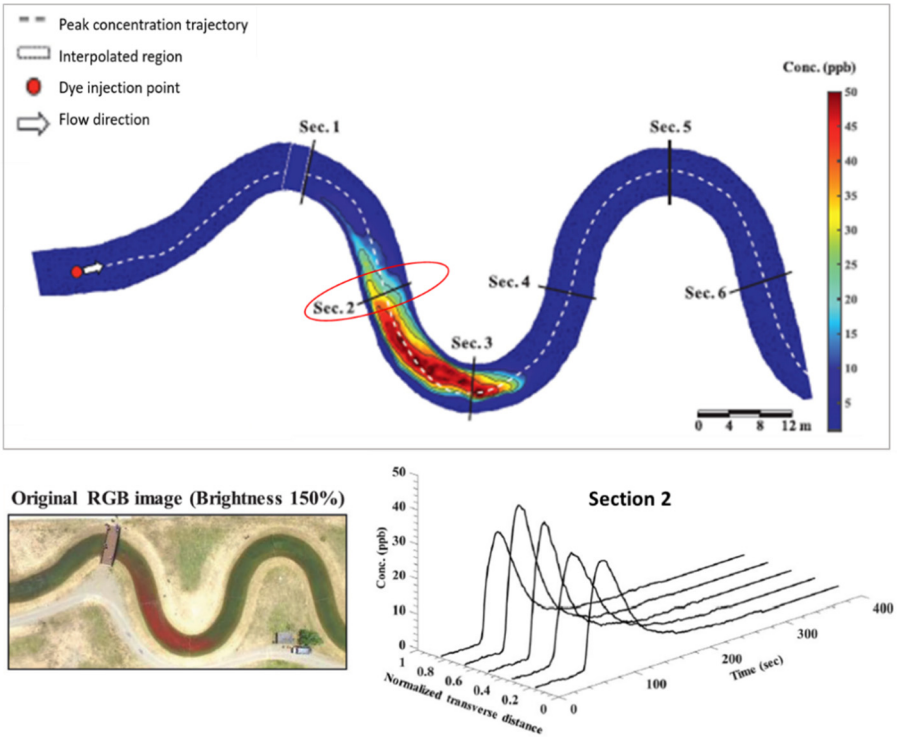

Figure 7. Transport of the tracer cloud at t = 90 s, original UAS RGB image and dye concentration distribution at Section 2. Modified from [122]. Copyright 2021 Advances in Water Resources.

Legleiter [123] assessed the suitability of various types of remotely sensed data (field spectra, hyperspectral images from manned and unmanned aircraft, and high resolution digital aerial photography) to estimate concentrations of a visible tracer. The results showed that a broad range of visible wavelengths were strongly correlated with dye concentration and therefore, tracer dispersion could be accurately mapped using RGB imagery.

4.6.2. Plastic Pollution

Similarly, the problem of plastic pollution in aquatic ecosystems has garnered widespread public and scientific attention. The rampant proliferation of plastics has led to explore the use of UAS in the evaluation and dynamics of plastics in the aquatic environment and to the development of numerous works on this issue. Several authors such as [124–126] have explored methodologies for the monitoring and automatic quantification of anthropogenic marine debris based on UAS imagery and machine learning

techniques. It should be noted however, that most of these studies have been conducted in marine and coastal environments and to date, only a few works focus on fluvial systems. Geraeds et al. [127] presented a novel methodology to quantify the floating riverine plastic transport in the Klang River, Malaysia. In order to make detailed cross-sectional plastic transport profiles, the authors conducted an aerial survey with flight transects perpendicular to the river flow direction. The flight path was set up at three different altitudes relative to the instantaneous water level. Depending on the altitude at which images were taken, they served different purposes. Although sudden changes in weather conditions can lead to a loss of accuracy in flight altitude, the authors documented similar plastic densities and transport profiles using UAS aerial surveys, visual observations and plastic sampling. Jakovljevic et al. [128] utilized high resolution orthophotos obtained from UAS and S*f*M algorithms to map floating plastics in rivers and lakes in Bosnia Herzegovina. The authors developed an end-to end semantic segmentation algorithm based on U-Net architecture that enabled to accurately detect and classify 3 types of plastic (OPS, Nylon and PET) at different spatial resolutions with an underestimation of the plastic area of only 3.4%. More recently, Hengstmann and Fischer [129] identified sources for plastics and influences on their distribution at four sandy bank border segments of Lake Tollense in Germany. They compared field-based observations with the results of anthropogenic litter detection via UAS imagery and obtained good recovery rates when minimizing the flight height. In addition, the aerial images were used to test automatic and supervised image analysis to detect and classify plastics.

4.7. Harmful Algal Blooms (HABs) and Eutrophication

Harmful algae blooms (HABs) outbreaks are closely linked to anthropogenic eutrophication and have dramatically increased in the past three decades. HABs not only give rise to a rapid depletion of dissolved oxygen in water bodies and massive deaths of aquatic organisms but can also pose a serious threat to human health owing to the production of neurotoxins of some species [130]. As in other disciplines, HAB monitoring evolved from expensive and labor-intensive water sampling techniques to satellite monitoring. However, HABs are highly dynamic and their monitoring, even with high resolution satellite data, is not always suitable owing to their limited temporal resolution (large time intervals between image re-acquisition). The quality of satellite images can be affected by weather conditions, cloudiness and atmospheric absorption. Remote sensing from manned aircrafts, nevertheless, can provide high spatio-temporal resolutions but its implementation is costly and usually limited by safety, logistical and operational issues. In this context, UAS offer the flight flexibility, temporal and spatial resolution and rapid response needed to detect and monitor HAB dynamics with minimal environmental disturbance. Despite these advantages, since the development of UAS-based techniques and the commercialization of suitable sensors is very recent, the current number of studies focused on the study of HABs with UAS is limited. One of the applications given to UAS imagery has been the visual inspection of water bodies, e.g., [131] detected the beginning of eutrophication process and tracked the proliferation of ragweed in a small lake in Hungary using high resolution photography from two different models of fixed wing UAS and an hexacopter.

Other early works include the use of conventional cameras separately or in combination with NIR sensors to map water quality and quantify algae concentrations. Ngo et al. [132] studied the relationship between algae concentration and water color through the implementation of a regression model. A RGB camera mounted on an UAS was used to capture videos and retrieve individual frames to subsequently extract the color component values of green and blue pixels. Van der Merwe and Price [133] exploited the contrast between clear water and cyanobacteria in color-infrared imagery. The authors employed UAS equipped with modified cameras that captured NIR and blue wavelengths to quantify algae densities at water surface through the formulation of a parameter termed as "blue normalized difference vegetation index". Their work emphasizes the role of UAS remote sensing as a complement to traditional methods and the usefulness of drones when HABs

need to be characterized and tracked with a high spatio-temporal precision and accuracy. Su and Chou [134] utilized UAS RGB and NIR imagery and established regression models to find the best correlations between water quality parameters and band ratio in order to map the trophic state of a small reservoir. The authors emphasized that, compared with traditional photogrammetry or satellite remote sensing techniques, UAS offer a better cost/profit ratio in terms of reservoir mapping. Jang et al. [135] monitored HABs in one of the largest rivers in South Korea and developed a modified Algal Bloom Detection Index that included the red band (625 nm) to better distinguish algal bloom from clear water. Their study combined the use of UASs equipped with a S110 RGB camera and a NIR camera with in situ measurements of spectral reflectance and water quality analysis. Aguirre-Gómez et al. [136] combined UAS high-definition imagery with in situ radiometric measurements and algae sampling to conduct spatio-temporal analysis of the extension and distribution of cyanobacteria in urban lakes of Mexico. Their approach included dark object subtraction techniques in order to correct sun/sky glint errors and proved to be an accurate, flexible and rapid method to detect and predict eutrophication and cyanobacterial blooms in reservoirs. Salarux and Kaewplang [137] employed UAS-derived RGB and NIR imagery to calculate vegetation indexes and assess their performance using mathematical models (Figure 8). This approach proved to be useful for estimating algal biomass.

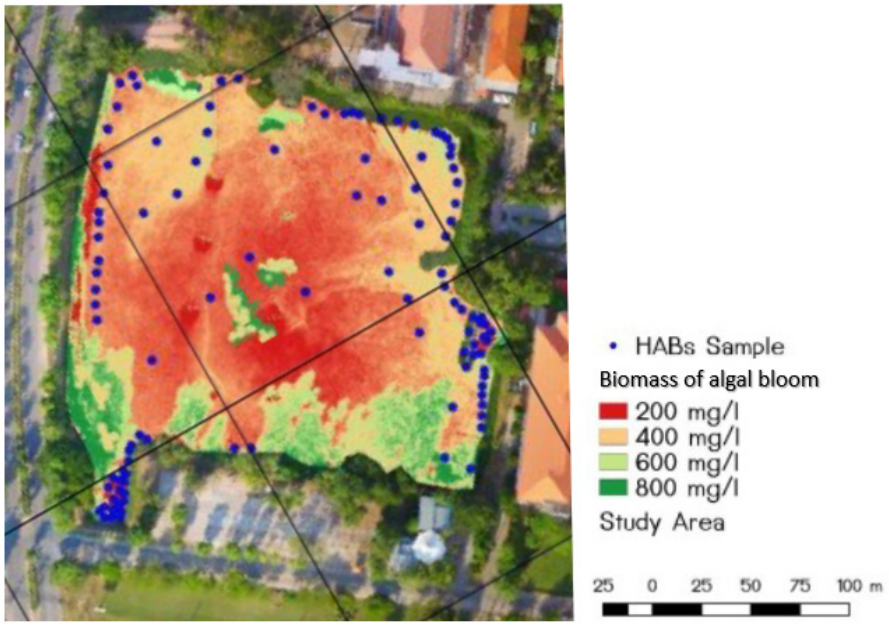

Figure 8. Map of algae biomass. Modified from [137].

Since the recent development of the first lightweight hyperspectral cameras adapted to be mounted on UASs, the applications of this type of imagery have increased in numerous research fields, including algal bloom monitoring. Although hyperspectral sensors are still expensive, these are emerging as alternatives to conventional RGB and multispectral cameras owing to their improved capacity of quantifying water constituents and identifying algal and phytoplankton groups species and genus by their spectral pigment absorption. Some recent experiences using drone-borne hyperspectral imagery can be cited; in an early work, Honkavaara et al. [138] presented a promising water quality monitoring technique that combined small-manned vehicles and UAS equipped with a Fabry-Perot interferometer (FPI) hyperspectral camera. Becker et al. [139] deployed two different low-cost UAS configurations in a lake and a river to monitor water quality and assess potential algal blooms in near-real time. UAS were equipped with hyperspectral radiometers to measure chlorophyll-a, cyanobacteria index, surface scums and suspended minerals. The UAS spectral data presented a quality similar to that from ground based spectroradiometers and enabled the construction of transect maps of derived cyanobacterial index products that

showed the distribution of algae abundance in the systems. Penmetcha et al. [140] proposed a deep learning-based algae detector and a multi-robot system algae removal planner integrated by an UAS and a USV. More recently, Castro et al. [38] presented a multisensor tool to monitor water quality in a Spanish reservoir affected by eutrophication. Their approach combined satellite, in situ data and multispectral UAS imagery to retrieve chl-a concentrations, which indicates the trophic status of the system. The performance of the different sensors, empirical models and band indices was evaluated. The authors concluded that multi-platform and multi-sensor approaches have great potential for small reservoir eutrophication monitoring. Kwon et al. [141] retrieved hyperspectral data from portable and drone-based sensors to develop bio-optical algorithms, measure the vertical pigment-concentration profile and map the distribution of phycocyanin in a deep reservoir. The bio-optical algorithms implemented using UAS-based reflectance measurements performed slightly worse than those using in situ remote sensing. The authors point out that future work should aim to improve remote-sensing algorithms through the identification of the relationship between pigment cumulation depth and light attenuation. Zhang et al. [142] mapped the concentration of eutrophication-related parameters in an urban river through the development of a self-adapting ANN based on UAS hyperspectral imagery and using the modified spectral reflectance of water measured with a ground-based analytical spectral device.

4.8. Water Sampling and In Situ Parameter Measurement

In addition to acquiring images, UAS are being increasingly used to take water samples, as they eliminate sampling risks to humans and allow to reach otherwise inaccessible locations. These innovative sampling platforms reduce costs and efforts, increasing the speed and range at which samples were traditionally obtained and allow to obtain undisturbed samples when hoovered at an adequate height to avoid induced mixing due to downwash. Some of the first references on the use of these instruments date correspond to Ore et al. [143] and Detweiler et al. [144], who designed a mechanism for sampling water autonomously from an UAS. The system was able to collect 3 samples of 20 mL per mission and the properties of the water collected matched that from manual samples, proving the adequacy of this technique. Similar works on the use of UAS as water sampling tools can be found in [145,146].

More recently, water sampling from UAS has gone a step further by including a wide range of sensors to conduct in situ measurements of different physical-chemical parameters. Song et al. [147] compared the reliability and effectiveness of UAS-based in situ physico-chemical measurements and water sampling with traditional and sensor-based methods. Although UAS enhance the reliability of data, there are still barriers to their full integration in limnological studies; the drone´s maximum carrying capacity limits the number and volume of samples, making these less representative of water chemistry compared to manually collected samples. Elijah et al. [148] implemented a smart river monitoring system that included an UAS to collect water samples and was equipped with and array of sensors and probes. Koparan et al. [149] designed a lightweight hexacopter equipped with a multiprobe system to measure temperature, electrical conductivity (EC), dissolved oxygen (DO), and pH. To avoid hoovering, the platform had flotation elements to allow the UAS to land on water surface at the waypoints in the flight mission. Esakki et al. [150] designed a UAS-based platform equipped with a robotic arm, a water pump and several sensors to collect 500 mL water samples and conduct in situ measurements of water quality. The results gathered by this system were in close agreement with laboratory test, with a 98% accuracy. To take samples of DNA fragments from a reservoir, Doi et al. [151] developed a new method for water collection consisting of a UAS with an attachment for a 1-L water bottle. The performance and contamination risk of the system was compared with that of samples obtained by boat, yielding similar results. Banerjee et al. [152] developed an electromechanical and pneumatic system to collect water samples from UAS, facilitating the access to inaccessible water bodies or dangerous mine sites and enabling the analysis of

several physical-chemical variables. Castendyk et al. [153] presented the first application of UASs for deep water sampling (up to 80 m) in pit lakes. Their system collected samples using Nisking sampler bottles and measured in situ the physical-chemical profiles of the water body. Later, Castendyk et al. [154] built on this work and on similar experiences to assess the state-of-the-art of drone water sampling of pit lakes in North America and to demonstrate how UAS-derived profiles can be used to select optimal sampling depths.

The use of UAS is not restricted to HAB monitoring and detection; in recent years UAS have also been employed to counteract them. Jung et al. [155] developed an autonomous robotic system to remove algal blooms that combined a catamaran-type USV instrumented with an electrocoagulation and flotation reactor with an UAS. The latter detected the HABs through an image-based algorithm and sent GPS coordinates to the USV for path planning. This method achieved a 98.3% of cyanobacteria removal.

Finally, the recent advances in technology have facilitated the creation of "multipurpose drones" that apart from completing standard tasks such as the acquisition of videos and photos, can monitor and take samples in a variety of environments and situations. An example of multipurpose UAS is provided by Agarwal et al. [156] who designed a platform capable of taking water samples, monitoring air and water quality in situ and that included video recording functions. Similarly, in order to access to an extreme environment such as the Lusi mud eruption in Indonesia, Di Stefano et al. [33] designed a multipurpose UAS. The platform was able to complete video surveys, high resolution photogrammetry, TIR mapping and was equipped with deployable thermometers and gas, mud and water samplers. An UAS equipped with a hydrophilic with a lipophilic balance (HLB), thin-film solid-phase microextraction (TF-SPME) sampler was developed by Grandy et al. [157] to remotely screen a wide range of pollutants present in water bodies. Finally, a recent review on drones use for water sampling can be found in [158].

5. UAS Applications in Hydrogeology

The number of papers documenting the application of UAS to groundwater (GW) and aquifer research is rather scarce, especially if compared with the extensive literature dealing with their use in riverine and oceanic environments. The reasons are the inherent limitations of remote sensing and the very early stage in which the technological developments in this field are currently. The major constraint in GW detection and mapping is related to the insufficient penetration capacity that remote sensing offers, only enabling the acquisition of data at the ground surface or within shallow subsurface layers a few meters deep. Apart from geophysical techniques, ground-penetrating radar (GPR) is the only technology that can survey depths of several meters. However, at present, owing to the mass, size and very high costs of these sensors, radars onboard UAS are still uncommon, and most experiences are restricted to applications such as landmine detection. Currently, some technological advances such as the Frequency Domain Electromagnetic (FDEM) method allow to perform geophysical surveys from UASs. These are aimed at the detection of underground properties such as magnetism and resistivity, which can be subsequently related with the presence of groundwater and its characteristics (e.g., salinity). Nevertheless, this field is still to be developed in scientific terms.

On the other hand, the thermal inertia of groundwater emergence in coastal areas (SGD) and fluvial systems has been recently exploited to generate temperature maps and monitor warm plumes by means of TIR-equipped UAS yielding promising results. Current available research on UASs applications in hydrogeology includes studies on surface-groundwater (SW–GW) exchange flow, submarine groundwater discharge (SGD), piezometric level delimitation and subsidence processes associated to groundwater withdrawals.

5.1. Surface Water–Groundwater (SW–GW) Interactions

Surface water–groundwater (SW–GW) interactions are critical to calculate water balances and sustainable levels of water extraction. These interactions have been traditionally

studied through an array of methods (e.g., differential gauging, seepage meters, tracer injection experiments, monitoring of piezometric heads or satellite remote sensing) whose selection depend on the temporal and spatial scale, limitations and uncertainties inherent to each technique. Recently, UAS have been implemented in SW–GW research since they are the only tools that enable indirect observations of these processes with a sufficiently high spatial resolution.

As several experiences have demonstrated, UAS-derived TIR imagery can provide useful information on the size and extent of groundwater plumes emerging from springs and near streambanks, especially when the temperature contrast between SW and GW is marked. Abolt et al. [159] mapped thermal refugia associated with groundwater discharge in Devil´s river (Texas) using a small UAS equipped with an inexpensive uncooled microbolometer and proposed a method for stabilizing the resulting image mosaic and compensating the pixel bias. This low-cost platform produced more consistent results than those obtained from a more expensive TIR camera system and allowed to generate high quality maps of surface temperature in riparian ecosystems.

TIR imagery has also been supported by optical products; Harvey et al. [160] evaluated the suitability of UAS equipped with lightweight TIR sensors to identify groundwater discharges and validate thermal refugia goals in a hydrological restored peatland. TIR, visible, and DSM products were compared to evaluate the landscape forms and thermal signature of groundwater inflows. The authors detected substantial inflows of warm groundwater that were visible along the restored channel, along with seepage areas, discrete seeps and thermally stable pools of ecological importance (Figure 9). This work emphasizes the usefulness of UAS-based TIR for mapping groundwater seeps in wetlands with a spatial coverage that is unimpeded by site-access considerations. However, the approach presents several limitations: Firstly, while the method proved to be effective in a continental climate with cold winter conditions, it is less effective when applied in spring, autumn or in temperate to tropical climates as the temperature contrast between SW–GW is less evident and becomes quickly lost by surface mixing. Secondly, TIR sensors cannot penetrate vegetation, meaning that surface waters may not always be visible because of foliage. Thirdly, shallow groundwater temperature can be similar to the mean annual surface temperature, weakening the TIR images contrast. Casas-Mulet et al. [161] generated high-resolution TIR and RGB orthomosaics to characterize cold water patches associated with groundwater inputs over a 95 km-long river section using simultaneous UAS flights. This method allowed to identify riverscape spatial patterns of temperature and to detect and classify these patches. Finally, UAS-based TIR has also been applied in the field of mining by Rautio et al. [162]. The authors combined airborne and UAS TIR imagery to identify SW–GW interactions for the planning and siting of mining facilities in order to prevent potential acid mine drainage pollution.

Other studies focused on SW–GW interactions rely on the combination of ground-based measurements, UAS photogrammetry and hydrologic modeling. Pai et al. [39] quantified sinuosity-driven GW-SW exchange in a river employing a suite of UAS-derived products (water surface elevation, normalized difference vegetation index (NDVI) maps and vegetation-top elevation distribution along meanders) and distributed in situ temperature measurements. *Sf*M photogrammetry was used to generate a DSM that allowed to estimate the river gradient, the hydraulic gradient across the meander necks, river-reach topography, and vegetation-top elevations. Compared with the surveyed ground control points, the modeled surface presented a 3.8 cm mean absolute error (less than aerial LiDAR) and a precision of 2.5 cm. The NDVI maps obtained presented a resolution better than 10 cm, enabling to document even individual plants. The combination of topographic analysis with low-cost multispectral imaging enabled to identify GW shortcutting, which occurred through the necks of the meander bends, where hydraulic gradients were found to be larger. Bandini et al. [163] evaluated the potential of spatially-distributed UASs observations for improving hydrological models and in particular, estimates of GW-SW exchange flow. The authors simulated a river and its catchment using an integrated hydro-

logical model that was calibrated through 2 methods; first, against river discharge retrieved by in situ stations and the piezometric head of the aquifers and second, against dense spatially distributed water level observations obtained with UASs. After calibration, the sharpness of the estimates of GW–SW time series improved by 50% using UASs and the root mean square error decreased by R75% compared with the values provided by the model calibrated against discharge only. Tang et al., [164] simulated a flood event with the groundwater model HydroGeosphere to study the spatial and temporal variability of riverbed topography and hydraulic conductivity on SW–GW exchange and groundwater heads. The authors combined several state-of-the-art techniques; UAS-based photogrammetry, physically based measurements and the ensemble Kalman Filter. This combination resulted in substantially improved hydrological predictions and enabled the estimation of river-aquifer fluxes. Briggs et al. [165] combined remote sensing with ground- and drone-based measurements to characterize the enhancement of SW–GW interactions and changes in water chemistry induced by beaver activity along two alluvial mountain streams in USA. Several UAS were deployed to map the river corridor and beaver ponds and *Sf*M techniques were applied to generate time-specific digital elevation models of floodplain structure and channel geomorphology. The UAS information was complemented with historical imagery, TIR data from handheld cameras and measurements of water quality (metals) and seepage associated to beaver pond return flows. The authors reported a multi-seasonal enhancement of the floodplain hydrologic connectivity and an increase in groundwater storage associated with beaver activity. Furlan et al. [166] combined electrical resistivity tomography with UAS photogrammetry to map the topography, internal morphology, water storage and hydrologic flow paths in a savanna wetland in Brazil. The authors used a fixed-wing UAS with a RGB sensor to obtain very high-resolution images and create an orthomosaic and a DSM for the relief analysis. The wetland was compartmentalized and the area and volume of each sector calculated for the subsequent hydrological modeling. On the other hand, the geophysical surveys provided information about groundwater behavior and infiltration zone architecture and enabled to produce a 2D inversion and a pseudo-3D model to visualize the subsurface geologic structure and hydrologic flow paths. The combined application of very high resolution UAS images and electrical surveys allowed the authors to propose a broader hydrologic interpretation of the wetland functioning and to complete surface and subsurface imaging of the system.

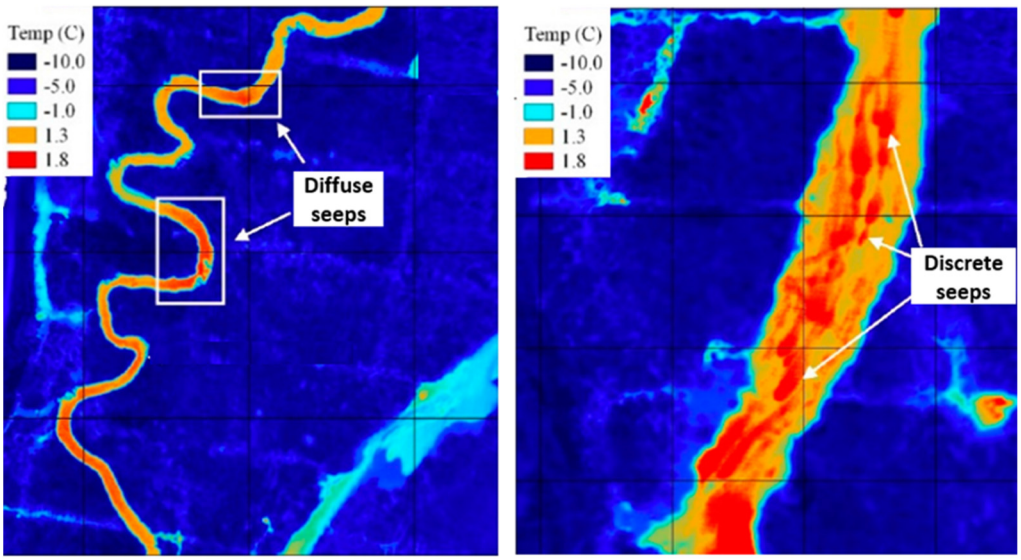

Figure 9. Thermal infrared (TIR) imagery showing the diffuse and discrete warm groundwater inputs into the stream. Modified from [160].

5.2. Submarine Groundwater Discharge (SGD) Mapping

Submarine groundwater discharge has a suggested impact on marine environment and geochemical cycles, playing a key role in the transport of nutrients, contaminants, and other chemical substances to coastal water. Although neglected for many years owing to the intrinsic difficulty of its quantification and the poor understanding of the process, in the last decades there has been a sharp increase in the number of publications on this topic. SGD has been traditionally studied using geochemical tracers, geophysical techniques, piezometric levels, water budgets and hydrological modeling. These classical methods, however, have large uncertainties associated, are labor-intensive and difficult to implement over large areas. Most SGD research is based on the detection of groundwater discharge from temperature anomalies and the seasonal contrast between ocean and groundwater temperature. TIR imagery from manned aircraft, although costly, has proved to be useful in mapping SGD, especially in areas where temperature contrasts between groundwater and seawater are marked. Conversely, satellite monitoring suffers either from an inadequate spatial resolution for detailed studies, or it is restricted by established schedules (revisit times) that may not be adequate for the needs of each study. In this context, since the implementation of UAS in SGD research is still relatively new, only a few recent studies are available, highlighting UAS´s suitability as affordable alternatives to the aforementioned methods and to overcome limitations in terms of spatial resolution.

Siebert [167] studied what they termed as "sub-lake groundwater discharges" in the Dead Sea; off-shore springs that drained the surrounding mountain freshwater aquifers. The authors integrated data obtained from ground-truth measurements, high-precision and high-resolution bathymetric campaigns, side-scan sonar imaging from an USV and imagery of sea surface temperature from a TIR sensor mounted on an UAS. Their approach proved to be suitable for precisely mapping SGD locations from remotely sensed thermal anomalies and even led the authors to hypothesize that the anomaly size reflects discharge quantities.

In a pioneer work, Lee et al. [168] successfully characterized and quantified SGD in an island of the Korean Peninsula through UAS-based TIR mapping supplemented by ground-based observations. Thermal signatures of SGD plumes and their tidal-derived fluctuations were captured with great detail (Figure 10).

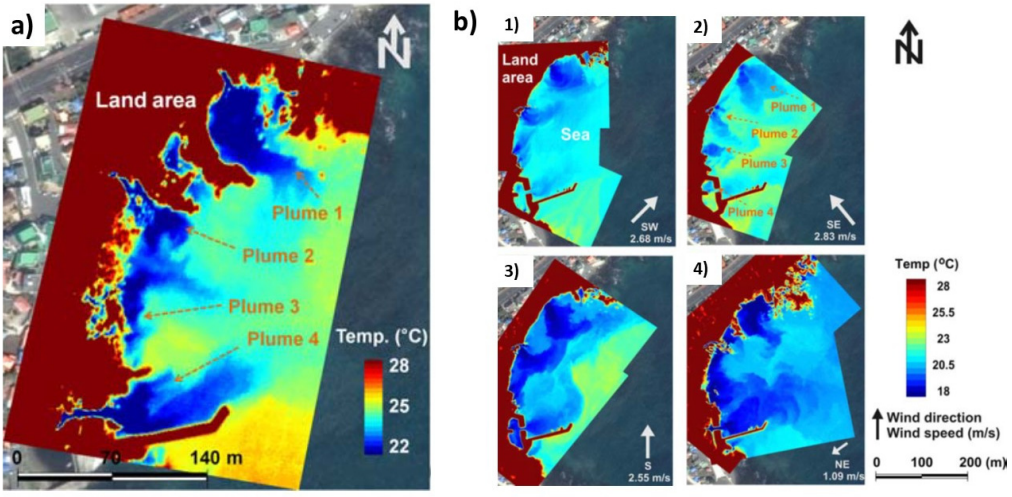

Figure 10. (**a**) Sea surface temperature maps and (**b1**–**4**) temperature fluctuations depending on the tidal stage (1. rising tide, 2. high tide, 3. outgoing tide and 4, low tide) captured by the UAS-based TIR. Extracted from [168].

This work evidenced that UASs offer better results in the study of SGD dynamics in small, localized target areas (0.01–1 km^2) than manned aircrafts, which are more adequate for regional characterizations. The drone-based methodology allows an easier control of

the spatial resolution, more flexibility in field operations and lower costs compared to conventional aerial surveys, making it a powerful tool to study SGD and other coastal processes.

More recently, Mallast and Siebert [44] investigated variations in thermal radiation induced by focused and diffuse SGD in a sedimentary fan of the Dead Sea. The authors used a hoovering UAS equipped with a long-wave TIR camera and a radiometry module and assumed that thermally stable areas indicated focused SGD whereas highly variable areas indicated diffuse SGD. After applying specific subjective variance thresholds and spatio-temporal analysis, their results highlighted that the spatio-temporal behavior of a SGD-induced thermal radiation pattern can vary in size and over time by up to 155% in the case of focused SGDs and by up to 600% in the case of diffuse SGDs owing to underlying flow dynamics. The authors recommend the application of this approach prior any in situ sampling in order to identify adequate sampling locations and intervals.

5.3. Water Table Definition

The definition of the water table of an aquifer is usually carried out from observations at specific points in the territory with the subsequent application of the interpolation methods devised for this purpose (linear, polynomial, IDW, kriging, etc.). Direct observations are made by measuring water level depth with specific instruments (electrical probes, pressure transducers, radar, etc.) at observation points that reach the saturated zone (wells, boreholes, piezometers, pits, excavations). The piezometric level is inferred from the subtraction of water level depth from ground elevation with respect to datum. Photogrammetry carried out from UAS can provide high accuracy in the definition of the morphology of the terrain and is useful for levelling the observation points. Nevertheless, the determination of the level depth using UAS require certain exposure of the water sheet. Therefore, it is not possible to detect the piezometric level when the observation points are closed (installed boreholes or piezometers with covers) or when their geometric characteristics (diameter) do not favor inspection from air. That is why there are very few works in this field. The only applications described refer to peatlands and karst aquifers affected by large dissolution/collapse structures (cenotes).

Thus, Rahman et al. [169] proposed a methodology for mapping groundwater in a treed-bog peatland using orthophotography and photogrammetric point clouds acquired from an UAS. DSM and a DEM were used to obtain a canopy height model and open water objects were converted into a continuous surface. The elevations of the samples were interpolated to generate a water table surface, which was then subtracted from the DEM to obtain the depth to water surface. This method demonstrated great potential for measuring groundwater levels over large, complex and inaccessible areas, although its performance and effectiveness were hindered in densely vegetated areas. Bandini et al. [170] proposed a methodology based on the observation from UAS to define the water surface elevation (WSE) in cenotes in the calcareous aquifer of the Yucatán Peninsula (Mexico), which is useful to feed hydrological models and estimate hydraulic gradients and groundwater flow directions. WSE observations were retrieved using a radar and a global navigation satellite system on-board a multicopter platform. Moreover, water depth was measured using a tethered floating sonar controlled by the UAS. Later, these observations are transformed to orthometric water height above mean sea level and compared with the ground-truth observations retrieved by a GNSS rover station. The authors estimate an accuracy better than 5–7 cm in the WSE and they highlight that UASs allow monitoring of remote areas located in the jungle, which are difficult to access by human operators.

Other applications related to the detection of the saturated zone depth using UAS are focused on the identification of drainage systems in agricultural fields; Allred et al. [171] conducted UAS surveys to detect drainage pipes in a pilot agricultural field where documentation on the pipe network was available. The study was caried out using visible, NIR, and TIR images during the dry period. Under these field conditions, drainage pipes could not be detected with the VIS and NIR imagery. Conversely, the TIR image detected

roughly 60% of the subsurface drainage infrastructure. Kratt et al. [172] followed a similar approach and obtained better results with visible images than with the TIR sensor, which did not detect the phenomenon owing to thermal differences lower than the sensitivity of the instrument, a consequence of non-optimal environmental conditions.

5.4. Subsidence

Subsidence is a slow and gradual movement caused by tension-induced changes over natural terrains or built surfaces. This geological hazard can affect all types of terrains and is produced by a range of natural factors and human activities. With regards to the latter, groundwater extraction plays a significant role in the occurrence of land subsidence; pumping can lead to substantial drawdowns and water table depressions in the neighboring areas of boreholes, resulting higher water extraction costs and, in the worst-case scenario, to material and human damage.

This phenomenon has been extensively documented worldwide using different techniques like interferometry synthetic aperture radar (InSAR) from satellites or numerical models [173–175]. Nowadays, the implementation of UASs as complements or enhancing tools for conventional surveying and mapping of subsidence is drawing increasing attention among the scientific community, however, this discipline is still in its earlier stages of development.

Although works on the application of UASs in the study of subsidence linked to groundwater extraction are scarce, some pioneering attempts are worth mentioning. One of them was conducted in Arizona (USAEE.UU), where the central and southeastern regions present subsidence problems driven by groundwater pumping, leading to fissures and cracks caused by tensile failure of sediment and soil. These fissures have resulted in property damages and increase the risk of groundwater contamination from surface pollutants. To address this issue, the Arizona Geological Survey (AZGS) founded the earth fissure program in 2007 to systematically identify, map, and monitor earth fissures. In 2018 the AZGS incorporated the use of UAS-*Sf*M for fissure monitoring and terrain mapping [176]. As a result, they produced accurate DSM of the areas affected by fissures, highlighted the diffuse nature of ground surface disturbance around fissure openings and proposed to extend the use of UASs to other zones of Arizona due to the better precision of the method. On the other hand, the effect of subsidence on groundwater levels has been studied by [177,178]. The authors used RGB images from a rotatory-wing UAS to extract subsided cultivated land in high-groundwater level coal mines. After calculating several vegetation indexes and applying a hierarchical extraction method to define subsided farmland, the comparison of the results of the UAS-based images (Kappa coefficient of 0.96) with a traditional method (Kappa coefficient of 0.86) demonstrated the highest accuracy of the former. However, the methodology displayed some weaknesses; although the remote sensing images obtained by UAS at low altitude had high spatial resolution, the amount of data was relatively large, slowing down data processing. In addition, the high energy demands of the rotary-wing UAS only allowed to conduct shorter flights, what hindered the obtention of data over larger areas, and the resolution of the images was affected by meteorological conditions (cloudiness and fog).

6. Results and Conclusions

6.1. Current Applications of UASs in Water Resource Research

The advent of UASs as remote sensing platforms for hydrological monitoring constitutes a major breakthrough in water research, overcoming the shortcomings of traditional manned-aircraft and satellite observations, and opening up new opportunities to achieve the spatio-temporal resolutions required to understand small-scale hydrological processes and dynamics. In this regard, UASs are bridging the gaps between satellites, airborne imagery and ground-based measurements. In addition, the increasingly competitive prices of these platforms, together with the parallel advances in sensor development and soft-

ware tools that automate data processing, have led to a growing interest of the scientific community on this technology.

In this paper a total of 122 research works is summarized, providing an overview on UASs recent advances and state-of-the-art methodologies implemented in the study of surface water and groundwater, including notions about the types of sensors, platforms and advantages and limitations of this technology that is in rapid and continuous development. The works reviewed were classified according to the phenomenon or process under study and the type of water body considered.

The number of studies focused on surface water notably exceeds those on groundwater investigations (Figure 11). In fact, UASs applications on surface water account for 84.4% of all the papers reviewed, of which river bathymetry and the study of floods are the prevalent studies. Conversely, groundwater research using aerial drones constitute only a 15.6% of the total, being most of these papers related to SW–GW interactions.

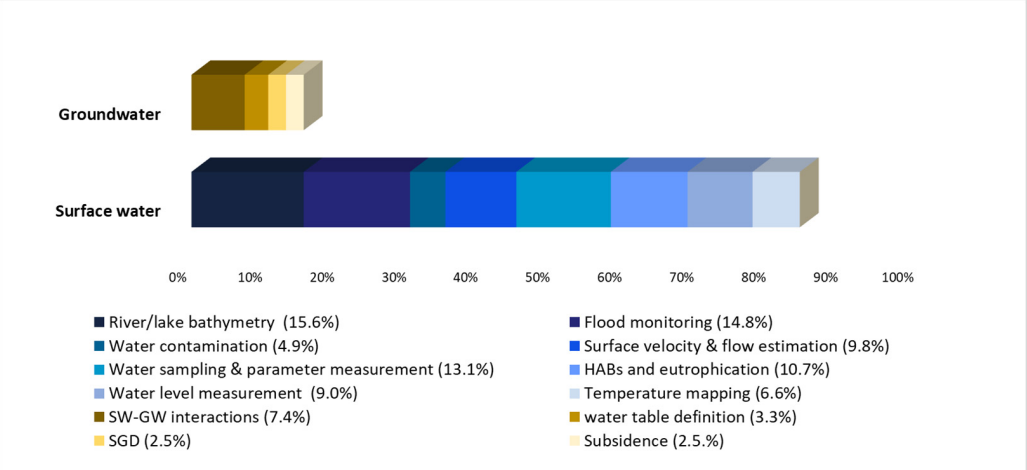

Figure 11. Percentage distribution and number of reviewed studies of UASs applications in hydrology.

As this review evidences, a wide number of approaches have been developed for observing surface and submerged features of rivers, lakes and other wetlands. For instance, UAS-based optical methods have been used to create bathymetric maps by stablishing correlations between pixel values or spectral properties of the images. The combination of UAS images and videos with optical velocimetry and particle tracking techniques have enabled to characterize surface flows and velocity fields of rivers and streams. UAS-derived data have been extensively used to produce high accuracy DEMs to identify the extent of inundations and improve flood models. IR sensors mounted on UASs have been also deployed to detect temperature patterns within rivers or lakes, and to identify groundwater inputs or warm effluents from power plants. Likewise, RGB, IR and more recently hyperspectral cameras are being deployed from UASs to early detect and monitor eutrophication and harmful algal blooms. Moreover, beyond being tools for the remotely acquisition of data, UAS have gone one step further, with devices that allow the collection of water samples and the measurement of parameters in situ, overcoming the many limitations of traditional manual sampling.

Nevertheless, the application of UAS technology to surface water research is subject to several limitations and challenges. Among the most obvious are the weather conditions, such as strong winds, rain, cloudiness and sunglint contamination that may hamper the flights and result in geometrically distorted images. These factors might degrade the quality of the images, making necessary the formulation of correction algorithms specific for the flight and environmental conditions. Likewise, the characteristics and distribution of vegetation can hinder the acquisition of data from the terrain in both aerial and underwater conditions and can even represent a serious risk for the movement and safety of unmanned aerial platforms. The accuracy in vertical and horizontal position (x,y,z

axis) is crucial in many studies and rely heavily on the GCP or the availability/accuracy of the IMU/INS/RTK units. In this regard, ensuring a good geolocation and alignment of UAS imagery in highly dynamic environments (e.g., rivers), areas with scarce ground control points or surfaces rich in contrast, constitutes another problematic aspect. Fortunately, the recent advances and miniaturization of differential GNSS are yielding significant improvements in flight performance both in terms of accuracy and integrity. Other indirect problem associated with the large body of information generated by UASs, is the high data storage and processing capacity needed. Additional constraints related to low payload capacity, which limits the number of sensors that can be mounted on the platform, short flight times and battery duration also requires previous consideration.

On the one hand, the implementation of UAS remote sensing to the study of underground environments and processes, hidden from direct observations, is even more challenging since this technology was initially devised to detect features directly from the sky. In this context, the main limitation is the insufficient penetration capacity that most remote sensing techniques (except for long wave radar) present beyond the uppermost soil layer. If conditions are favorable and in the absence of vegetation, long wave radar imagery can detect groundwater levels situated a few meters deep. Although the application of UAS remote sensing to groundwater exploration is limited by technological development, several recent studies demonstrate the usefulness of this technique and represent a promising step forward in the knowledge of these water bodies. Most of these works are based on the detection of groundwater-induced thermal anomalies in coastal waters or riverine systems to characterize plumes and produce temperature maps. On the other hand, a few studies have taken advantage of the particular configuration of certain areas such as cenotes and peatlands to map water table. A research field currently under development is the use of geophysical instruments from UASs for the detection or characterization of groundwater (e.g., the aforementioned FDEM).

Regarding the types of UASs employed in hydrological research, as Tables 4 and 5 show, the prevalent type was rotary-wing, both in surface water and groundwater, although fixed wing and other types (paraglider) were also reported. The reason is that, even though fixed-wing UAS can cover larger areas and offer longer flight times, rotary wings allow greater maneuverability, allowing vertical movements and hoovering, as well as working in inaccessible areas, which are characteristic often needed in many data collection tasks. However, some authors have made a combined use of both types of platforms in order to complement their strengths and compensate for their weaknesses. Among the 122 works reviewed, 10 did not specify the type or model of UAS used and were excluded from tables.

Table 4. Number of reviewed works by UAS type in surface water research.

	Bathymetry	Water Level	Surface Velocity/Discharge	Flood Monitoring	TermperaTure Mapping	Water Contamination	HABs	Water Sampling	Sum
Fixed-wing	1	1	0	10	2	0	2	0	16
Rotary-wing	17	9	12	6	6	5	8	14	77
Both	0	0	0	2	0	0	2	0	4
Other	1	0	0	0	0	0	0	0	1

Table 5. Number of reviewed works by UAS type in groundwater research.

	SW–GW Interactions	SGD	Water Table Definition	Subsidence	Sum
Fixed-wing	1	0	1	0	2
Rotary-wing	4	2	3	3	12
Both	0	0	0	0	0

6.2. UAS Application in Freshwater Research: Future Prospects

Since their recent emergence in the civil sphere, UASs have been subject to continuous improvements and innovations developed in parallel with advances in sensors. Their incorporation into the research field has opened a new era in remote data acquisition, with a range of applications that is continuously growing.

UASs are providing researchers and water managers the opportunity of gathering exceptionally large data volumes in a safe, cost-effective and relatively easier manner than traditional methods. In fact, UASs have come to revolutionize measurement and sampling campaigns and, owing to their unprecedent spatio-temporal coverage and the recent advances in sensor technologies that allow to capture surface and submerged processes, it is possible to analyze aquatic systems from a holistic point of view more than ever. In a period of just two decades, UASs have deeply transformed the discipline of hydrology and its use alone or in combination with other instruments have contributed to the generation of highly accurate representations of fluvial morphology, to map surface properties and study system´s interactions.

In addition, UASs have rapidly evolved from early prototypes like balloons, paragliders and paramotors to sophisticated lightweight platforms able to operate in difficult to reach and hazardous environments preventing risks for operators. The decreasing prices of the electronic components and the many possibilities available in terms of platform customization and sensor combination have democratized their use and made them affordable even for small research groups and modest institutions.

In the light of the broad literature selection presented here, there are several opportunities and challenges that need to be considered for the full and efficient implementation of UAS in hydrological research and management:

Platform limitations: The use of non-metric cameras and the development of low-cost platforms have been a key in the rapid uptake of UASs for the obtention of high-resolution data on demand. However, UASs are subject to a number of limitations. Among the most important and evident ones, is UAS maximum payload, which have hindered their coupling with certain sensors and storage devices so far (e.g., to date there are only a few commercially available models of LiDAR sensors compatible with UAS). This limitation has prevented drones from carrying more integrated systems with multiple sensors, data processing equipment and communication hardware. Another hurdle of this technology is UAS´s high energy requirements (an inherent issue of scaling down the vehicle), which limit their autonomy, spatial coverage and makes necessary to interrupt the flight multiple times to replace batteries. In addition, most UASs cannot fly autonomously without GPS and may not be deployed under adverse meteorological conditions, situation that is recently changing with the development of new industrial ratings (e.g., IP44 and IP45) that ensure protection against debris and water. The widespread and more effective implementation of UASs in research calls for further miniaturization of components, the development of alternative power sources such as thin-film photovoltaic panels or tethered systems that extend the battery duration and provide a reliable wired communication, and improvements in vehicle autonomy, minimizing human intervention.

Methodological robustness: The many papers reviewed here reflect the necessity of increasing research efforts and carrying out more experiences on the application of UASs in hydrology, with a special focus on groundwater. While some applications based on visual imagery to extract river morphology, bathymetry or flood extents have gathered highly accurate results, other methods such as multispectral approaches to infer water quality, TIR imagery to study fluvial temperature patterns, video data to estimate stream flow or UAS-based approaches to define water table are still subject to important limitations. These methodologies will have to be refined as UAS and sensing technologies mature and optimized processing tools and algorithms are developed.

Information gaps: The availability of detailed hydrological information at global scale is still uneven in terms of spatial distribution and type of data. Thus, we believe that future research efforts should aim at increasing the current collection of UAS imagery

over different types of basins, hydrological conditions and events, with especial focus on ungauged systems and information-scarce areas. On the other hand, as this review evidences, most UAS remote sensing techniques are focused on morphological aspects, while works on dynamic processes such water surface elevation, discharge estimations and surface-groundwater interactions are less common owing to technological, spatial and temporal limitations. In this regard, future advances in the field of UASs, together with multiplatform and multisensor approaches will narrow these information voids and will enable a deeper understanding of water bodies functioning and interactions.

Image processing and the role of machine learning: Manual extraction of regions of interest from the large volumes of information generated by UASs is a costly and time demanding task, even more in long-term monitoring programs involving repeated surveys. In this context, the emergence of machine learning algorithms provides great opportunities to automatize image processing workflows and address the challenges of hydrological research. To date, some works have successfully implemented machine learning approaches such as support vector machine or ANN for feature extraction and classification, or to solve non-linear problems in hydrological forecasting. Nevertheless, despite machine learning usually outperforms physically based models, their predictive accuracy is restricted to the range of input data used in the training stage. Thus, a long-term goal to improve model predictions at broader scales is to fill information gaps and acquire consistent spatial-temporal hydrological input data for their subsequent integration into artificial intelligence networks. As technology matures, UASs will be extremely useful tools for the acquisition of different types of training data.

Uneven legal framework: The rapid expansion of UASs has not been balanced by an exhaustive regulation and to date, there is not a single harmonized regulatory instrument at international scale. This situation stems from the shift in the use of UAS technology from the initial military purpose to professional/commercial and recreational use, leading to new legal implications. UASs must comply with principles of safety and privacy and every activity performed by a drone is subject to a convoluted set of specific sectorial rules such as data protection, privacy law, aviation law, telecommunication law, environmental law, product liability or criminal law, which hinders the potential and competitiveness of the drone market. The integration of civil UAS into all areas of the airspace while removing the technical barriers that limit their flight and addressing the inherent security, privacy and ethical issues still one of the main obstacles to overcome. Recently, the European Regulation 2019/947 [179] on the rules and procedures for the operation and registration of unmanned aircraft has constituted a leap forward in the unification and integration of civil drones into all areas of the airspace. The document sets the rules for conducting operational risk assessment and cross-border operations within the EU, the conditions under which drone operations can be allowed and establishes the requirements for the registration of UAS operators and certified UAS among others.

Finally, this paper presents a comprehensive literature review on the diverse applications of UAS in the fields of hydrology and hydrogeology, classifying them according to the aim of the study and covering a range of aspects such as the types of platforms and sensors used, their strengths, limitations and the new possibilities opened up by their combination with other measurement instruments. The compilation of experiences here summarized has demonstrated the great supporting role of UASs to ground-based and satellite-borne observations, covering the demand of near real-time and cost-effective data especially in the study of highly dynamic processes. Despite the rapid advances experienced and all the advantages UASs offer, their integration in water resource research (as in many other research fields) it is still in its infancy; there is room for improvement in many aspects such as image processing, standardization of the techniques and procedures adopted, or UASs integration with traditional instruments and analysis tools. In this regard, experience and data sharing among researchers can further improve hydrological research, help to fill knowledge gaps and lay the foundations for the design of methodologies and protocols appropriate to different hydrological contexts. This review aims at serving as a reference or

introductory document for all the researchers and water managers who are interested in embracing this novel technology to meet their needs and to unify in a single document all the possibilities, potential approaches and the results obtained by different authors through the implementation of UASs.

Author Contributions: Conceptualization, M.V.-N., S.G.-L. and L.B.; methodology, M.V.-N., S.G.-L. and L.B.; investigation, M.V.-N., S.G.-L., V.R.-O. and Á.S.-B.; data curation, M.V.-N., S.G.-L., V.R.-O. and Á.S.-B.; writing—original draft preparation, M.V.-N. and S.G.-L.; writing—review and editing, L.B., V.R.-O. and Á.S.-B.; supervision, S.G.-L. All authors have read and agreed to the published version of the manuscript.

Funding: This work has received financial support from the research group RNM373 Geoscience-UCA of Junta de Andalucía.

Institutional Review Board Statement: Not applicable.

Informed Consent Statement: Not applicable.

Data Availability Statement: No new data were created or analyzed in this study. Data sharing is not applicable to this article.

Acknowledgments: The authors want to thank the support received from the plan "Programa de Fomento e Impulso de la Investigación y Transferencia" of the University of Cádiz. The authors also want to express their gratitude to the reviewers and in particular, to Ulf Mallast, whose encouraging and insightful comments have greatly contributed to improve this review. We also thank the Drone Service of the University of Cádiz, which kindly lent their equipment to illustrate this work and to the infrastructure project EQC2018-004446-P of the Ministry of Economy and Competitiveness of the Government of Spain.

Conflicts of Interest: The authors declare no conflict of interests.

References

1. WWAP (UNESCO World Water Assessment Programme). *The United Nations World Water Development Report 2019: Leaving No One Behind*; UNESCO: Paris, France, 2019.
2. IPCC. *Climate Change 2014: Synthesis Report. Contribution of Working Groups I, II and III to the Fifth Assessment Report of the Intergovernmental Panel on Climate Change*; Core Writing Team, Pachauri, R.K., Meyer, L.A., Eds.; IPCC: Geneva, Switzerland, 2014; 151p.
3. Chamoso, P.; González-Briones, A.; Rivas, A.; De Mata, F.B.; Corchado, J.M. The Use of Drones in Spain: Towards a Platform for Controlling UAVs in Urban Environments. *Sensors* **2018**, *18*, 1416. [CrossRef] [PubMed]
4. Linchant, J.; Lisein, J.; Semeki, J.; Lejeune, P.; Vermeulen, C. Are unmanned aircraft systems (UASs) the future of wildlife monitoring? A review of accomplishments and challenges. *Mammal Rev.* **2015**, *45*, 239–252. [CrossRef]
5. Chabot, D.; Bird, D.M. Wildlife research and management methods in the 21st century: Where do unmanned aircraft fit in? *J. Unmanned Veh. Syst.* **2015**, *3*, 137–155. [CrossRef]
6. Christie, K.S.; Gilbert, S.L.; Brown, C.L.; Hatfield, M.; Hanson, L. Unmanned aircraft systems in wildlife research: Current and future applications of a transformative technology. *Front. Ecol. Environ.* **2016**, *14*, 241–251. [CrossRef]
7. Adão, T.; Hruška, J.; Pádua, L.; Bessa, J.; Peres, E.; Morais, R.; Sousa, J.J. Hyperspectral Imaging: A Review on UAV-Based Sensors, Data Processing and Applications for Agriculture and Forestry. *Remote Sens.* **2017**, *9*, 1110. [CrossRef]
8. Wieser, M.; Mandlburger, G.; Hollaus, M.; Otepka, J.; Glira, P.; Pfeifer, N. A Case Study of UAS Borne Laser Scanning for Measurement of Tree Stem Diameter. *Remote Sens.* **2017**, *9*, 1154. [CrossRef]
9. Radoglou-Grammatikis, P.; Sarigiannidis, P.; Lagkas, T.; Moscholios, I. A compilation of UAV applications for precision agriculture. *Comput. Netw.* **2020**, *172*, 107148. [CrossRef]
10. Rakha, T.; Gorodetsky, A. Review of Unmanned Aerial System (UAS) applications in the built environment: Towards automated building inspection procedures using drones. *Autom. Constr.* **2018**, *93*, 252–264. [CrossRef]
11. Zhou, S.; Gheisari, M. Unmanned aerial system applications in construction: A systematic review. *Constr. Innov.* **2018**, *18*, 453–468. [CrossRef]
12. Restas, A. Drone Applications for Supporting Disaster Management. *World J. Eng. Technol.* **2015**, *3*, 316–321. [CrossRef]
13. McCabe, M.; Rodell, M.; Alsdorf, D.; Miralles, D.; Uijlenhoet, R.; Wagner, W.; Lucieer, A.; Houborg, R.; Verhoest, N.; Franz, T.; et al. The future of earth observation in Hydrology. *Air Space Eur.* **2017**, *2*, 42–44. [CrossRef]
14. Debell, L.; Anderson, K.; Brazier, R.; King, N.; Jones, L. Water resource management at catchment scales using lightweight UAVs: Current capabilities and future perspectives. *J. Unmanned Veh. Syst.* **2016**, *4*, 7–30. [CrossRef]

15. Colomina, I.; Molina, P. Unmanned aerial systems for photogrammetry and remote sensing: A review. *ISPRS J. Photogramm. Remote Sens.* **2014**, *92*, 79–97. [CrossRef]
16. Carrivick, J.L.; Smith, M.W. Fluvial and aquatic applications of Structure from Motion photogrammetry and unmanned aerial vehicle/drone technology. *Wiley Interdiscip. Rev. Water* **2019**, *6*, e1328. [CrossRef]
17. Tomsett, C.; Leyland, J. Remote sensing of river corridors: A review of current trends and future directions. *River Res. Appl.* **2019**, *35*, 779–803. [CrossRef]
18. Rhee, D.S.; Kim, Y.D.; Kang, B.; Kim, D. Applications of unmanned aerial vehicles in fluvial remote sensing: An overview of recent achievements. *KSCE J. Civ. Eng.* **2017**, *22*, 588–602. [CrossRef]
19. Kislik, C.; Dronova, I.; Kelly, M. UAVs in Support of Algal Bloom Research: A Review of Current Applications and Future Opportunities. *Drones* **2018**, *2*, 35. [CrossRef]
20. Wu, D.; Li, R.; Zhang, F.; Liu, J. A review on drone-based harmful algae blooms monitoring. *Environ. Monit. Assess.* **2019**, *191*, 211. [CrossRef] [PubMed]
21. Terwilliger, B.; Ison, D.C.; Robbins, J.; Vincenzi, D. *Small Unmanned Aircraft Systems Guide: Exploring Designs, Operations, Regulations, and Economics*; Aviation Supplies & Academics: Washington, DC, USA, 2017.
22. Arjomandi, M.; Agostino, S.; Mammone, M.; Nelson, M.; Zhou, T. *Classification of Unmanned Aerial Vehicles*; Mech. Eng.; University of Adelaide: Adelaide, Australia, 2006.
23. Weibel, R.E.; Hansman, R.J. Safety considerations for operation of different classes of UAVs in the NAS. In Proceedings of the Aiaa 4th Aviation Technology, Integration and Operations (Atio) Forum, Chicago, IL, USA, 20–22 September 2004; Volume 1, pp. 341–351. [CrossRef]
24. Hassanalian, M.; Abdelkefi, A. Classifications, applications, and design challenges of drones: A review. *Prog. Aerosp. Sci.* **2017**, *91*, 99–131. [CrossRef]
25. Watts, A.C.; Ambrosia, V.G.; Hinkley, E.A. Unmanned Aircraft Systems in Remote Sensing and Scientific Research: Classification and Considerations of Use. *Remote Sens.* **2012**, *4*, 1671–1692. [CrossRef]
26. Johnston, D.W. Unoccupied Aircraft Systems in Marine Science and Conservation. *Annu. Rev. Mar. Sci.* **2019**, *11*, 439–463. [CrossRef]
27. Boukoberine, M.N.; Zhou, Z.; Benbouzid, M. A critical review on unmanned aerial vehicles power supply and energy management: Solutions, strategies, and prospects. *Appl. Energy* **2019**, *255*, 113823. [CrossRef]
28. Snavely, N.; Seitz, S.M.; Szeliski, R. Modeling the World from Internet Photo Collections. *Int. J. Comput. Vis.* **2008**, *80*, 189–210. [CrossRef]
29. He, Y.; Weng, Q. *High Spatial Resolution Remote Sensing: Data, Analysis, and Applications*; CRC Press: Boca Raton, FL, USA, 2018; ISBN 9781498767682.
30. Dugdale, S.J. A practitioner's guide to thermal infrared remote sensing of rivers and streams: Recent advances, precautions and considerations. *Wiley Interdiscip. Rev. Water* **2016**, *3*, 251–268. [CrossRef]
31. Mesas-Carrascosa, F.-J.; Pérez-Porras, F.; De Larriva, J.E.M.; Frau, C.M.; Agüera-Vega, F.; Carvajal-Ramírez, F.; Martínez-Carricondo, P.; García-Ferrer, A. Drift Correction of Lightweight Microbolometer Thermal Sensors On-Board Unmanned Aerial Vehicles. *Remote Sens.* **2018**, *10*, 615. [CrossRef]
32. Döpper, V.; Gränzig, T.; Kleinschmit, B.; Förster, M. Challenges in UAS-Based TIR Imagery Processing: Image Alignment and Uncertainty Quantification. *Remote Sens.* **2020**, *12*, 1552. [CrossRef]
33. Di Stefano, G.; Romeo, G.; Mazzini, A.; Iarocci, A.; Hadi, S.; Pelphrey, S. The Lusi drone: A multidisciplinary tool to access extreme environments. *Mar. Pet. Geol.* **2018**, *90*, 26–37. [CrossRef]
34. Lejot, J.; Delacourt, C.; Piégay, H.; Fournier, T.; Trémélo, M.-L.; Allemand, P. Very high spatial resolution imagery for channel bathymetry and topography from an unmanned mapping controlled platform. *Earth Surf. Process. Landf.* **2007**, *32*, 1705–1725. [CrossRef]
35. Woodget, A.S.; Dietrich, J.T.; Wilson, R.T. Quantifying Below-Water Fluvial Geomorphic Change: The Implications of Refraction Correction, Water Surface Elevations, and Spatially Variable Error. *Remote Sens.* **2019**, *11*, 2415. [CrossRef]
36. Gentile, V.; Mróz, M.; Spitoni, M.; Lejot, J.; Piégay, H.; Demarchi, L. Bathymetric Mapping of Shallow Rivers with UAV Hyperspectral Data. In Proceedings of the Fifth International Conference on Telecommunications and Remote Sensing, Milan, Italy, 10–11 October 2016; pp. 43–49.
37. Flener, C.; Vaaja, M.; Jaakkola, A.; Krooks, A.; Kaartinen, H.; Kukko, A.; Kasvi, E.; Hyyppä, H.; Hyyppä, J.; Alho, P. Seamless Mapping of River Channels at High Resolution Using Mobile LiDAR and UAV-Photography. *Remote Sens.* **2013**, *5*, 6382–6407. [CrossRef]
38. Castro, C.C.; Gómez, J.A.D.; Martín, J.D.; Sánchez, B.A.H.; Arango, J.L.C.; Tuya, F.A.C.; Díaz-Varela, R. An UAV and Satellite Multispectral Data Approach to Monitor Water Quality in Small Reservoirs. *Remote Sens.* **2020**, *12*, 1514. [CrossRef]
39. Pai, H.; Malenda, H.F.; Briggs, M.A.; Singha, K.; González-Pinzón, R.; Gooseff, M.N.; Tyler, S.W. Potential for Small Unmanned Aircraft Systems Applications for Identifying Groundwater-Surface Water Exchange in a Meandering River Reach. *Geophys. Res. Lett.* **2017**, *44*, 11868–11877. [CrossRef]
40. Legleiter, C.J.; Harrison, L.R. Remote Sensing of River Bathymetry: Evaluating a Range of Sensors, Platforms, and Algorithms on the Upper Sacramento River, California, USA. *Water Resour. Res.* **2019**, *55*, 2142–2169. [CrossRef]

41. Collas, F.P.; Van Iersel, W.K.; Straatsma, M.W.; Buijse, A.D.; Leuven, R.S. Sub-Daily Temperature Heterogeneity in a Side Channel and the Influence on Habitat Suitability of Freshwater Fish. *Remote Sens.* **2019**, *11*, 2367. [CrossRef]
42. Dugdale, S.J.; Kelleher, C.A.; Malcolm, I.A.; Caldwell, S.; Hannah, D.M. Assessing the potential of drone-based thermal infrared imagery for quantifying river temperature heterogeneity. *Hydrol. Process.* **2019**, *33*, 1152–1163. [CrossRef]
43. Kinzel, P.J.; Legleiter, C.J. sUAS-Based Remote Sensing of River Discharge Using Thermal Particle Image Velocimetry and Bathymetric Lidar. *Remote Sens.* **2019**, *11*, 2317. [CrossRef]
44. Mallast, U.; Siebert, C. Combining continuous spatial and temporal scales for SGD investigations using UAV-based thermal infrared measurements. *Hydrol. Earth Syst. Sci.* **2019**, *23*, 1375–1392. [CrossRef]
45. Chen, S.; Johnson, F.; Drummond, C.; Glamore, W. A new method to improve the accuracy of remotely sensed data for wetland water balance estimates. *J. Hydrol. Reg. Stud.* **2020**, *29*, 100689. [CrossRef]
46. Vázquez-Tarrío, D.; Borgniet, L.; Liébault, F.; Recking, A. Using UAS optical imagery and SfM photogrammetry to characterize the surface grain size of gravel bars in a braided river (Vénéon River, French Alps). *Geomorphology* **2017**, *285*, 94–105. [CrossRef]
47. Li, H.; Chen, L.; Wang, Z.; Yu, Z. Mapping of River Terraces with Low-Cost UAS Based Structure-from-Motion Photogrammetry in a Complex Terrain Setting. *Remote Sens.* **2019**, *11*, 464. [CrossRef]
48. Hemmelder, S.; Marra, W.; Markies, H.; De Jong, S.M. Monitoring river morphology & bank erosion using UAV imagery—A case study of the river Buëch, Hautes-Alpes, France. *Int. J. Appl. Earth Obs. Geoinf.* **2018**, *73*, 428–437. [CrossRef]
49. Mazzoleni, M.; Paron, P.; Reali, A.; Juizo, D.; Manane, J.; Brandimarte, L. Testing UAV-derived topography for hydraulic modelling in a tropical environment. *Nat. Hazards* **2020**, *103*, 139–163. [CrossRef]
50. Zinke, P.; Flenner, C. 2013. Experiences from the use of Unmanned Aerial Vehicles (UAV) for River Bathymetry Modelling in Norway. *Vann* **2013**, *48*, 351–360.
51. Woodget, A.S.; Carbonneau, P.E.; Visser, F.; Maddock, I.P. Quantifying submerged fluvial topography using hyperspatial resolution UAS imagery and structure from motion photogrammetry. *Earth Surf. Process. Landf.* **2014**, *40*, 47–64. [CrossRef]
52. Dietrich, J.T. Bathymetric Structure-from-Motion: Extracting shallow stream bathymetry from multi-view stereo photogrammetry. *Earth Surf. Process. Landf.* **2017**, *42*, 355–364. [CrossRef]
53. Entwistle, N.S.; Heritage, G.L. Small unmanned aerial model accuracy for photogrammetrical fluvial bathymetric survey. *J. Appl. Remote Sens.* **2019**, *13*, 014523. [CrossRef]
54. Partama, I.Y.; Kanno, A.; Ueda, M.; Akamatsu, Y.; Inui, R.; Sekine, M.; Yamamoto, K.; Imai, T.; Higuchi, T. Removal of water-surface reflection effects with a temporal minimum filter for UAV-based shallow-water photogrammetry. *Earth Surf. Process. Landf.* **2018**, *43*, 2673–2682. [CrossRef]
55. Skarlatos, D.; Agrafiotis, P. A Novel Iterative Water Refraction Correction Algorithm for Use in Structure from Motion Photogrammetric Pipeline. *J. Mar. Sci. Eng.* **2018**, *6*, 77. [CrossRef]
56. Agrafiotis, P.; Karantzalos, K.; Georgopoulos, A.; Skarlatos, D. Correcting Image Refraction: Towards Accurate Aerial Image-Based Bathymetry Mapping in Shallow Waters. *Remote Sens.* **2020**, *12*, 322. [CrossRef]
57. Agrafiotis, P.; Skarlatos, D.; Georgopoulos, A.; Karantzalos, K. DepthLearn: Learning to Correct the Refraction on Point Clouds Derived from Aerial Imagery for Accurate Dense Shallow Water Bathymetry Based on SVMs-Fusion with LiDAR Point Clouds. *Remote Sens.* **2019**, *11*, 2225. [CrossRef]
58. Mandlburger, G.; Pfennigbauer, M.; Schwarz, R.; Flöry, S.; Nussbaumer, L. Concept and Performance Evaluation of a Novel UAV-Borne Topo-Bathymetric LiDAR Sensor. *Remote Sens.* **2020**, *12*, 986. [CrossRef]
59. Kasvi, E.; Salmela, J.; Lotsari, E.; Kumpula, T.; Lane, S. Comparison of remote sensing based approaches for mapping bathymetry of shallow, clear water rivers. *Geomorphology* **2019**, *333*, 180–197. [CrossRef]
60. Erena, M.; Atenza, J.F.; García-Galiano, S.; Domínguez, J.A.; Bernabé, J.M. Use of Drones for the Topo-Bathymetric Monitoring of the Reservoirs of the Segura River Basin. *Water* **2019**, *11*, 445. [CrossRef]
61. Bandini, F.; Olesen, D.; Jakobsen, J.; Kittel, C.M.M.; Wang, S.; Garcia, M.; Bauer-Gottwein, P. Technical note: Bathymetry observations of inland water bodies using a tethered single-beam sonar controlled by an unmanned aerial vehicle. *Hydrol. Earth Syst. Sci.* **2018**, *22*, 4165–4181. [CrossRef]
62. Alvarez, L.V.; Moreno, H.A.; Segales, A.R.; Pham, T.G.; Pillar-Little, E.A.; Chilson, P.B. Merging Unmanned Aerial Systems (UAS) Imagery and Echo Soundings with an Adaptive Sampling Technique for Bathymetric Surveys. *Remote Sens.* **2018**, *10*, 1362. [CrossRef]
63. Kim, J.S.; Baek, D.; Seo, I.W.; Shin, J. Retrieving shallow stream bathymetry from UAV-assisted RGB imagery using a geospatial regression method. *Geomorphology* **2019**, *341*, 102–114. [CrossRef]
64. Langhammer, J.; Janský, B.; Kocum, J.; Minařík, R. 3-D reconstruction of an abandoned montane reservoir using UAV photogrammetry, aerial LiDAR and field survey. *Appl. Geogr.* **2018**, *98*, 9–21. [CrossRef]
65. Tamminga, A.D.; Hugenholtz, C.H.; Eaton, B.C.; Lapointe, M. Hyperspatial Remote Sensing of Channel Reach Morphology and Hydraulic Fish Habitat Using an Unmanned Aerial Vehicle (UAV): A First Assessment in the Context of River Research and Management. *River Res. Appl.* **2015**, *31*, 379–391. [CrossRef]
66. Templin, T.; Popielarczyk, D.; Kosecki, R. Application of Low-Cost Fixed-Wing UAV for Inland Lakes Shoreline Investigation. *Pure Appl. Geophys.* **2018**, *175*, 3263–3283. [CrossRef]
67. Alsdorf, D.E.; Rodríguez, E.; Lettenmaier, D.P. Measuring surface water from space. *Rev. Geophys.* **2007**, *45*. [CrossRef]
68. Ridolfi, E.; Manciola, P. Water Level Measurements from Drones: A Pilot Case Study at a Dam Site. *Water* **2018**, *10*, 297. [CrossRef]

69. Gao, A.; Wu, S.; Wang, F.; Wu, X.; Xu, P.; Yu, L.; Zhu, S. A Newly Developed Unmanned Aerial Vehicle (UAV) Imagery Based Technology for Field Measurement of Water Level. *Water* **2019**, *11*, 124. [CrossRef]
70. Bandini, F.; Jakobsen, J.; Olesen, D.H.; Reyna-Gutierrez, J.A.; Bauer-Gottwein, P. Measuring water level in rivers and lakes from lightweight Unmanned Aerial Vehicles. *J. Hydrol.* **2017**, *548*, 237–250. [CrossRef]
71. Bandini, F.; Sunding, T.P.; Linde, J.; Smith, O.; Jensen, I.K.; Köppl, C.J.; Butts, M.; Bauer-Gottwein, P. Unmanned Aerial System (UAS) observations of water surface elevation in a small stream: Comparison of radar altimetry, LIDAR and photogrammetry techniques. *Remote Sens. Environ.* **2020**, *237*, 111487. [CrossRef]
72. Jiang, L.; Bandini, F.; Smith, O.; Jensen, I.K.; Bauer-Gottwein, P. The Value of Distributed High-Resolution UAV-Borne Observations of Water Surface Elevation for River Management and Hydrodynamic Modeling. *Remote Sens.* **2020**, *12*, 1171. [CrossRef]
73. Tymków, P.; Jóźków, G.; Walicka, A.; Karpina, M.; Borkowski, A. Identification of Water Body Extent Based on Remote Sensing Data Collected with Unmanned Aerial Vehicle. *Water* **2019**, *11*, 338. [CrossRef]
74. Niedzielski, T.; Witek, M.; Spallek, W. Observing river stages using unmanned aerial vehicles. *Hydrol. Earth Syst. Sci.* **2016**, *20*, 3193–3205. [CrossRef]
75. García-López, S.; Ruiz-Ortiz, V.; Barbero, L.; Sánchez-Bellón, Á. Contribution of the UAS to the determination of the water budget in a coastal wetland: A case study in the natural park of the Bay of Cádiz (SW Spain). *Eur. J. Remote Sens.* **2018**, *51*, 965–977. [CrossRef]
76. Mohamad, N.; Khanan, M.F.A.; Ahmad, A.; Din, A.H.M.; Shahabi, H. Evaluating Water Level Changes at Different Tidal Phases Using UAV Photogrammetry and GNSS Vertical Data. *Sensors* **2019**, *19*, 3778. [CrossRef]
77. Yucel, M.A.; Turan, R.Y. Areal Change Detection and 3D Modeling of Mine Lakes Using High-Resolution Unmanned Aerial Vehicle Images. *Arab. J. Sci. Eng.* **2016**, *41*, 4867–4878. [CrossRef]
78. McGlynn, B.L.; Blöschl, G.; Borga, M.; Bormann, H.; Hurkmans, R.; Komma, J.; Nandagiri, L.; Uijlenhoet, R.; Wagener, T. *A Data Acquisition Framework for Runoff Prediction in Ungauged Basins, Runoff Prediction in Ungauged Basins*; Cambridge University Press: Cambridge, UK, 2013. [CrossRef]
79. Mishra, A.K.; Coulibaly, P. Developments in hydrometric network design: A review. *Rev. Geophys.* **2009**, *47*. [CrossRef]
80. Sichangi, A.W.; Wang, L.; Yang, K.; Chen, D.; Wang, Z.; Li, X.; Zhou, J.; Liu, W.; Kuria, D. Estimating continental river basin discharges using multiple remote sensing data sets. *Remote Sens. Environ.* **2016**, *179*, 36–53. [CrossRef]
81. Sneeuw, N.; Lorenz, C.; Devaraju, B.; Tourian, M.J.; Riegger, J.; Kunstmann, H.; Bárdossy, A. Estimating Runoff Using Hydro-Geodetic Approaches. *Surv. Geophys.* **2014**, *35*, 1333–1359. [CrossRef]
82. Yang, S.; Wang, J.; Wang, P.; Gong, T.; Liu, H. Low Altitude Unmanned Aerial Vehicles (UAVs) and Satellite Remote Sensing Are Used to Calculated River Discharge Attenuation Coefficients of Ungauged Catchments in Arid Desert. *Water* **2019**, *11*, 2633. [CrossRef]
83. Yang, S.; Wang, P.; Lou, H.; Wang, J.; Zhao, C.; Gong, T. Estimating River Discharges in Ungauged Catchments Using the Slope–Area Method and Unmanned Aerial Vehicle. *Water* **2019**, *11*, 2361. [CrossRef]
84. Lou, H.; Wang, P.; Yang, S.; Hao, F.; Ren, X.; Wang, Y.; Shi, L.; Wang, J.; Gong, T. Combining and Comparing an Unmanned Aerial Vehicle and Multiple Remote Sensing Satellites to Calculate Long-Term River Discharge in an Ungauged Water Source Region on the Tibetan Plateau. *Remote Sens.* **2020**, *12*, 2155. [CrossRef]
85. Koutalakis, P.; Tzoraki, O.; Zaimes, G. UAVs for Hydrologic Scopes: Application of a Low-Cost UAV to Estimate Surface Water Velocity by Using Three Different Image-Based Methods. *Drones* **2019**, *3*, 14. [CrossRef]
86. Pearce, S.; Ljubičić, R.; Peña-Haro, S.; Perks, M.; Tauro, F.; Pizarro, A.; Sasso, S.F.D.; Strelnikova, D.; Grimaldi, S.; Maddock, I.; et al. An Evaluation of Image Velocimetry Techniques under Low Flow Conditions and High Seeding Densities Using Unmanned Aerial Systems. *Remote Sens.* **2020**, *12*, 232. [CrossRef]
87. Tauro, F.; Pagano, C.; Phamduy, P.; Grimaldi, S.; Porfiri, M. Large-Scale Particle Image Velocimetry From an Unmanned Aerial Vehicle. *IEEE/ASME Trans. Mechatronics* **2015**, *20*, 3269–3275. [CrossRef]
88. Tauro, F.; Porfiri, M.; Grimaldi, S. Surface flow measurements from drones. *J. Hydrol.* **2016**, *540*, 240–245. [CrossRef]
89. Lewis, Q.W.; Lindroth, E.M.; Rhoads, B.L. Integrating unmanned aerial systems and LSPIV for rapid, cost-effective stream gauging. *J. Hydrol.* **2018**, *560*, 230–246. [CrossRef]
90. Sasso, S.F.D.; Pizarro, A.; Manfreda, S. Metrics for the Quantification of Seeding Characteristics to Enhance Image Velocimetry Performance in Rivers. *Remote Sens.* **2020**, *12*, 1789. [CrossRef]
91. Thumser, P.; Haas, C.; Tuhtan, J.A.; Fuentes-Pérez, J.F.; Toming, G. RAPTOR-UAV: Real-time particle tracking in rivers using an unmanned aerial vehicle. *Earth Surf. Process. Landf.* **2017**, *42*, 2439–2446. [CrossRef]
92. Fulton, J.; Anderson, I.; Chiu, C.-L.; Sommer, W.; Adams, J.; Moramarco, T.; Bjerklie, D.; Fulford, J.; Sloan, J.; Best, H.; et al. QCam: sUAS-Based Doppler Radar for Measuring River Discharge. *Remote Sens.* **2020**, *12*, 3317. [CrossRef]
93. Dyer, J.L.; Moorhead, R.J.; Hathcock, L. Identification and Analysis of Microscale Hydrologic Flood Impacts Using Unmanned Aerial Systems. *Remote Sens.* **2020**, *12*, 1549. [CrossRef]
94. Mourato, S.; Fernandez, P.; Pereira, L.; Moreira, M. Improving a DSM Obtained by Unmanned Aerial Vehicles for Flood Modelling. *IOP Conf. Series: Earth Environ. Sci.* **2017**, *95*, 022014. [CrossRef]
95. Muthusamy, M.; Casado, M.R.; Salmoral, G.; Irvine, T.; Leinster, P. A Remote Sensing Based Integrated Approach to Quantify the Impact of Fluvial and Pluvial Flooding in an Urban Catchment. *Remote Sens.* **2019**, *11*, 577. [CrossRef]

96. Şerban, G.; Rus, I.; Vele, D.; Breţcan, P.; Alexe, M.; Petrea, D. Flood-prone area delimitation using UAV technology, in the areas hard-to-reach for classic aircrafts: Case study in the north-east of Apuseni Mountains, Transylvania. *Nat. Hazards* **2016**, *82*, 1817–1832. [CrossRef]
97. Yalcin, E. Two-dimensional hydrodynamic modelling for urban flood risk assessment using unmanned aerial vehicle imagery: A case study of Kirsehir, Turkey. *J. Flood Risk Manag.* **2018**, *12*, e12499. [CrossRef]
98. Özcan, O. Multi-temporal UAV based repeat monitoring of rivers sensitive to flood. *J. Maps* **2020**, 1–8. [CrossRef]
99. Diakakis, M.; Andreadakis, E.; Nikolopoulos, E.; Spyrou, N.; Gogou, M.; Deligiannakis, G.; Katsetsiadou, N.; Antoniadis, Z.; Melaki, M.; Georgakopoulos, A.; et al. An integrated approach of ground and aerial observations in flash flood disaster investigations. The case of the 2017 Mandra flash flood in Greece. *Int. J. Disaster Risk Reduct.* **2019**, *33*, 290–309. [CrossRef]
100. Leitão, J.P.; De Vitry, M.M.; Scheidegger, A.; Rieckermann, J. Assessing the quality of digital elevation models obtained from mini unmanned aerial vehicles for overland flow modelling in urban areas. *Hydrol. Earth Syst. Sci.* **2016**, *20*, 1637–1653. [CrossRef]
101. Hashemi-Beni, L.; Jones, J.; Thompson, G.; Johnson, C.; Gebrehiwot, A. Challenges and Opportunities for UAV-Based Digital Elevation Model Generation for Flood-Risk Management: A Case of Princeville, North Carolina. *Sensors* **2018**, *18*, 3843. [CrossRef]
102. Schumann, G.J.P.; Muhlhausen, J.; Andreadis, K.M. Rapid mapping of small-scale river-floodplain environments using UAV SfM supports classical theory. *Remote Sens.* **2019**, *11*, 982. [CrossRef]
103. Annis, A.; Nardi, F.; Petroselli, A.; Apollonio, C.; Arcangeletti, E.; Tauro, F.; Belli, C.; Bianconi, R.; Grimaldi, S. UAV-DEMs for Small-Scale Flood Hazard Mapping. *Water* **2020**, *12*, 1717. [CrossRef]
104. Villanueva, J.R.E.; Martínez, L.I.; Montiel, J.I.P. DEM Generation from Fixed-Wing UAV Imaging and LiDAR-Derived Ground Control Points for Flood Estimations. *Sensors* **2019**, *19*, 3205. [CrossRef] [PubMed]
105. Tamminga, A.D.; Eaton, B.C.; Hugenholtz, C.H. UAS-based remote sensing of fluvial change following an extreme flood event. *Earth Surf. Process. Landf.* **2015**, *40*, 1464–1476. [CrossRef]
106. Abdelkader, M.; Shaqura, M.; Claudel, C.G.; Gueaieb, W. A UAV based system for real time flash flood monitoring in desert environments using Lagrangian microsensors. In Proceedings of the 2013 International Conference on Unmanned Aircraft Systems (ICUAS), Atlanta, GA, USA, 28–31 May 2013; pp. 25–34.
107. Popescu, D.; Ichim, L.; Stoican, F. Unmanned Aerial Vehicle Systems for Remote Estimation of Flooded Areas Based on Complex Image Processing. *Sensors* **2017**, *17*, 446. [CrossRef]
108. Gebrehiwot, A.; Hashemi-Beni, L.; Thompson, G.; Kordjamshidi, P.; Langan, T.E. Deep Convolutional Neural Network for Flood Extent Mapping Using Unmanned Aerial Vehicles Data. *Sensors* **2019**, *19*, 1486. [CrossRef]
109. Jakovljevic, G.; Govedarica, M.; Alvarez-Taboada, F.; Pajic, V. Accuracy Assessment of Deep Learning Based Classification of LiDAR and UAV Points Clouds for DTM Creation and Flood Risk Mapping. *Geosciences* **2019**, *9*, 323. [CrossRef]
110. Erdelj, M.; Natalizio, E.; Chowdhury, K.R.; Akyildiz, I.F. Help from the Sky: Leveraging UAVs for Disaster Management. *IEEE Pervasive Comput.* **2017**, *16*, 24–32. [CrossRef]
111. Salmoral, G.; Casado, M.R.; Muthusamy, M.; Butler, D.; Menon, P.P.; Leinster, P. Guidelines for the Use of Unmanned Aerial Systems in Flood Emergency Response. *Water* **2020**, *12*, 521. [CrossRef]
112. Kastridis, A.; Kirkenidis, C.; Sapountzis, M. An integrated approach of flash flood analysis in ungauged Mediterranean watersheds using post-flood surveys and unmanned aerial vehicles. *Hydrol. Process.* **2020**, *34*, 4920–4939. [CrossRef]
113. Handcock, R.N.; Torgersen, C.E.; Cherkauer, K.A.; Gillespie, A.R.; Tockner, K.; Faux, R.N.; Tan, J. Thermal Infrared Remote Sensing of Water Temperature in Riverine Landscapes. *Fluv. Remote Sens. Sci. Manag.* **2012**, *1*, 85–113. [CrossRef]
114. Jensen, A.M.; Neilson, B.T.; McKee, M.; Chen, Y. Thermal remote sensing with an autonomous unmanned aerial remote sensing platform for surface stream temperatures. *2012 IEEE Int. Geosci. Remote Sens. Symp.* **2012**, 5049–5052. [CrossRef]
115. Wawrzyniak, V.; Piégay, H.; Allemand, P.; Vaudor, L.; Grandjean, P. Prediction of water temperature heterogeneity of braided rivers using very high resolution thermal infrared (TIR) images. *Int. J. Remote Sens.* **2013**, *34*, 4812–4831. [CrossRef]
116. Kelly, J.; Kljun, N.; Olsson, P.-O.; Mihai, L.; Liljeblad, B.; Weslien, P.; Klemedtsson, L.; Eklundh, L. Challenges and Best Practices for Deriving Temperature Data from an Uncalibrated UAV Thermal Infrared Camera. *Remote Sens.* **2019**, *11*, 567. [CrossRef]
117. Chung, M.; Detweiler, C.; Hamilton, M.; Higgins, J.; Ore, J.-P.; Thompson, S. Obtaining the Thermal Structure of Lakes from the Air. *Water* **2015**, *7*, 6467–6482. [CrossRef]
118. Koparan, C.; Koc, A.B.; Sawyer, C.; Privette, C. Temperature Profiling of Waterbodies with a UAV-Integrated Sensor Subsystem. *Drones* **2020**, *4*, 35. [CrossRef]
119. Demario, A.; Lopez, P.; Plewka, E.; Wix, R.; Xia, H.; Zamora, E.; Gessler, D.; Yalin, A.P. Water Plume Temperature Measurements by an Unmanned Aerial System (UAS). *Sensors* **2017**, *17*, 306. [CrossRef] [PubMed]
120. Caldwell, S.; Kelleher, C.; Baker, E.; Lautz, L. Relative information from thermal infrared imagery via unoccupied aerial vehicle informs simulations and spatially-distributed assessments of stream temperature. *Sci. Total. Environ.* **2019**, *661*, 364–374. [CrossRef]
121. Powers, C.; Hanlon, R.; Schmale, D. Tracking of a Fluorescent Dye in a Freshwater Lake with an Unmanned Surface Vehicle and an Unmanned Aircraft System. *Remote Sens.* **2018**, *10*, 81. [CrossRef]
122. Baek, D.; Seo, I.W.; Kim, J.S.; Nelson, J.M. UAV-based measurements of spatio-temporal concentration distributions of fluorescent tracers in open channel flows. *Adv. Water Resour.* **2019**, *127*, 76–88. [CrossRef]
123. Legleiter, C.J.; McDonald, R.R.; Nelson, J.M.; Kinzel, P.J.; Perroy, R.L.; Baek, D.; Seo, I.W. Remote sensing of tracer dye concentrations to support dispersion studies in river channels. *J. Ecohydraulics* **2019**, *4*, 131–146. [CrossRef]

124. Martin, C.; Parkes, S.; Zhang, Q.; Zhang, X.; McCabe, M.F.; Duarte, C.M. Use of unmanned aerial vehicles for efficient beach litter monitoring. *Mar. Pollut. Bull.* **2018**, *131*, 662–673. [CrossRef] [PubMed]
125. Fallati, L.; Polidori, A.; Salvatore, C.; Saponari, L.; Savini, A.; Galli, P. Anthropogenic Marine Debris assessment with Unmanned Aerial Vehicle imagery and deep learning: A case study along the beaches of the Republic of Maldives. *Sci. Total Environ.* **2019**, *693*, 133581. [CrossRef] [PubMed]
126. Kako, S.; Morita, S.; Taneda, T. Estimation of plastic marine debris volumes on beaches using unmanned aerial vehicles and image processing based on deep learning. *Mar. Pollut. Bull.* **2020**, *155*, 111127. [CrossRef]
127. Geraeds, M.; Van Emmerik, T.; De Vries, R.; Bin Ab Razak, M.S. Riverine Plastic Litter Monitoring Using Unmanned Aerial Vehicles (UAVs). *Remote Sens.* **2019**, *11*, 2045. [CrossRef]
128. Jakovljevic, G.; Govedarica, M.; Alvarez-Taboada, F. A Deep Learning Model for Automatic Plastic Mapping Using Unmanned Aerial Vehicle (UAV) Data. *Remote Sens.* **2020**, *12*, 1515. [CrossRef]
129. Hengstmann, E.; Fischer, E.K. Anthropogenic litter in freshwater environments—Study on lake beaches evaluating marine guidelines and aerial imaging. *Environ. Res.* **2020**, *189*, 109945. [CrossRef]
130. Wurtsbaugh, W.A.; Paerl, H.W.; Dodds, W.K. Nutrients, eutrophication and harmful algal blooms along the freshwater to marine continuum. *Wiley Interdiscip. Rev. Water* **2019**, *6*. [CrossRef]
131. Fráter, T.; Juzsakova, T.; Lauer, J.; Dióssy, L.; Rédey, Á. Unmanned Aerial Vehicles in Environmental Monitoring—An Efficient Way for Remote Sensing. *J. Environ. Sci. Eng. A* **2015**, *4*, 85–91. [CrossRef]
132. Ngo, A.S.K.; Desingco, J.D.B.; Ii, M.O.C.; Uy, R.L.; Ong, P.M.B.; Punzalan, E.R.; Ilao, J.P. Determining the Correlation between Concentration Levels and the Visual Determining the Correlation Between Concentration Levels and the Visual Features of Algae in Water Surfaces. 2015. Available online: https://www.researchgate.net/publication/283086583_Determining_the_Correlation_Between_Concentration_Levels_and_the_Visual_Features_of_Algae_in_Water_Surfaces (accessed on 30 November 2020).
133. Van Der Merwe, D.; Price, K.P. Harmful Algal Bloom Characterization at Ultra-High Spatial and Temporal Resolution Using Small Unmanned Aircraft Systems. *Toxins* **2015**, *7*, 1065–1078. [CrossRef] [PubMed]
134. Su, T.-C.; Chou, H.-T. Application of Multispectral Sensors Carried on Unmanned Aerial Vehicle (UAV) to Trophic State Mapping of Small Reservoirs: A Case Study of Tain-Pu Reservoir in Kinmen, Taiwan. *Remote Sens.* **2015**, *7*, 10078–10097. [CrossRef]
135. Jang, S.W.; Yoon, H.J.; Kwak, S.N.; Sohn, B.Y.; Kim, S.G.; Kim, D.H. Algal Bloom Monitoring using UAVs Imagery. *Next Gener. Comput. Inf. Technol.* **2016**, *138*, 30–33. [CrossRef]
136. Aguirre-Gómez, R.; Salmerón-García, O.; Gómez-Rodríguez, G.; Peralta-Higuera, A. Use of unmanned aerial vehicles and remote sensors in urban lakes studies in Mexico. *Int. J. Remote Sens.* **2016**, *38*, 2771–2779. [CrossRef]
137. Salarux, C.; Kaewplang, S. Estimation of Algal Bloom Biomass Using UAV-Based Remote Sensing with NDVI and GRVI. *Mahasarakham Int. J. Eng. Technol.* **2020**, *6*, 1–6.
138. Honkavaara, E.; Hakala, T.; Kirjasniemi, J.; Lindfors, A.; Mäkynen, J.; Nurminen, K.; Ruokokoski, P.; Saari, H.; Markelin, L. New light-weight stereosopic spectrometric airborne imaging technology for high-resolution environmental remote sensing; case studies in water quality mapping. *ISPRS Int. Arch. Photogramm. Remote Sens. Spat. Inf. Sci.* **2013**, *XL-1/W1*, 139–144. [CrossRef]
139. Becker, R.H.; Sayers, M.; Dehm, D.; Shuchman, R.; Quintero, K.; Bosse, K.; Sawtell, R. Unmanned aerial system based spectroradiometer for monitoring harmful algal blooms: A new paradigm in water quality monitoring. *J. Great Lakes Res.* **2019**, *45*, 444–453. [CrossRef]
140. Penmetcha, M.; Luo, S.; Samantaray, A.; DIetz, J.E.; Yang, B.; Min, B.C. Computer vision-based algae removal planner for multi-robot teams. In Proceedings of the 2019 IEEE International Conference on Systems, Man and Cybernetics (SMC), Bari, Italy, 6–9 October 2019; pp. 1575–1581. [CrossRef]
141. Kwon, Y.S.; Pyo, J.; Duan, H.; Cho, K.H.; Park, Y. Drone-based hyperspectral remote sensing of cyanobacteria using vertical cumulative pigment concentration in a deep reservoir. *Remote Sens. Environ.* **2020**, *236*, 111517. [CrossRef]
142. Zhang, Y.; Wu, L.; Ren, H.; Liu, Y.; Zheng, Y.; Liu, Y.; Dong, J. Mapping Water Quality Parameters in Urban Rivers from Hyperspectral Images Using a New Self-Adapting Selection of Multiple Artificial Neural Networks. *Remote Sens.* **2020**, *12*, 336. [CrossRef]
143. Ore, J.P.; Elbaum, S.; Burgin, A.; Detweiler, C. Autonomous aerial water sampling. In *Field and Service Robotics*; Mejias, L., Corke, P., Roberts, J., Eds.; Springer International Publishing: Cham, Switzerland, 2015; pp. 137–151.
144. Detweiler, C.; Ore, J.-P.; Anthony, D.; Elbaum, S.; Burgin, A.J.; Lorenz, A. Environmental Reviews and Case Studies: Bringing Unmanned Aerial Systems Closer to the Environment. *Environ. Pract.* **2015**, *17*, 188–200. [CrossRef]
145. Schwarzbach, M.; Laiacker, M.; Mulero-Pazmany, M.; Kondak, K. Remote water sampling using flying robots. In Proceedings of the 2014 International conference on unmanned aircraft systems (ICUAS), Orlando, FL, USA, 27–30 May 2014; pp. 72–76. [CrossRef]
146. Terada, A.; Morita, Y.; Hashimoto, T.; Mori, T.; Ohba, T.; Yaguchi, M.; Kanda, W. Water sampling using a drone at Yugama crater lake, Kusatsu-Shirane volcano, Japan. *Earth Planets Space* **2018**, *70*, 64. [CrossRef]
147. Song, K.; Brewer, A.; Ahmadian, S.; Shankar, A.; Detweiler, C.; Burgin, A.J. Using unmanned aerial vehicles to sample aquatic ecosystems. *Limnol. Oceanogr. Methods* **2017**, *15*, 1021–1030. [CrossRef]
148. Elijah, O.; Rahman, T.A.; Leow, C.Y.; Yeen, H.C.; Sarijari, M.A.; Aris, A.; Salleh, J.; Chua, T.H. A concept paper on smart river monitoring system for sustainability in river. *Int. J. Integr. Eng.* **2018**, *10*, 130–139. [CrossRef]

149. Koparan, C.; Koc, A.B.; Privette, C.V.; Sawyer, C.B. In Situ Water Quality Measurements Using an Unmanned Aerial Vehicle (UAV) System. *Water* **2018**, *10*, 264. [CrossRef]
150. Esakki, B.; Ganesan, S.; Mathiyazhagan, S.; Ramasubramanian, K.; Gnanasekaran, B.; Son, B.; Park, S.W.; Choi, J.S. Design of Amphibious Vehicle for Unmanned Mission in Water Quality Monitoring Using Internet of Things. *Sensors* **2018**, *18*, 3318. [CrossRef]
151. Doi, H.; Akamatsu, Y.; Watanabe, Y.; Goto, M.; Inui, R.; Katano, I.; Nagano, M.; Takahara, T.; Minamoto, T. Water sampling for environmental DNA surveys by using an unmanned aerial vehicle. *Limnol. Oceanogr. Methods* **2017**, *15*, 939–944. [CrossRef]
152. Banerjee, B.; Raval, S.; Maslin, T.J.; Timms, W. Development of a UAV-mounted system for remotely collecting mine water samples. *Int. J. Mining Reclam. Environ.* **2018**, *34*, 385–396. [CrossRef]
153. Castendyk, D.; Straight, B.; Flllatreault, P.; Thlbeault, S.; Cameron, L. Aerial drones used to sample pit lake water reduce costs and improve safety. *Miner. Eng.* **2017**, *69*, 20–28.
154. Castendyk, D.; Straight, B.; Voorhis, J.; Somogyi, M.; Jepson, W.; Kucera, B. Using aerial drones to select sample depths in pit lakes. In Proceedings of the 13th International Conference on Mine Closure, Perth, Australia, 3–5 September 2019; pp. 1113–1126. [CrossRef]
155. Jung, S.; Cho, H.; Kim, N.; Kim, K.; Han, J.-I.; Myung, H. Development of Algal Bloom Removal System Using Unmanned Aerial Vehicle and Surface Vehicle. *IEEE Access* **2017**, *5*, 22166–22176. [CrossRef]
156. Agarwal, P.; Singh, M.K. A multipurpose drone for water sampling video surveillance. In Proceedings of the 2019 Second International Conference on Advanced Computational and Communication Paradigms (ICACCP), Gangtok, India, 25–28 February 2019; pp. 1–5. [CrossRef]
157. Grandy, J.J.; Galpin, V.; Singh, V.; Pawliszyn, J. Development of a Drone-Based Thin-Film Solid-Phase Microextraction Water Sampler to Facilitate On-Site Screening of Environmental Pollutants. *Anal. Chem.* **2020**, *92*, 12917–12924. [CrossRef] [PubMed]
158. Lally, H.; O'Connor, I.; Jensen, O.; Graham, C. Can drones be used to conduct water sampling in aquatic environments? A review. *Sci. Total Environ.* **2019**, *670*, 569–575. [CrossRef] [PubMed]
159. Abolt, C.; Caldwell, T.; Wolaver, B.; Pai, H. Unmanned aerial vehicle-based monitoring of groundwater inputs to surface waters using an economical thermal infrared camera. *Opt. Eng.* **2018**, *57*, 053113. [CrossRef]
160. Harvey, M.C.; Hare, D.K.; Hackman, A.; Davenport, G.; Haynes, A.B.; Helton, A.; Lane, J.J.W.; Briggs, M.A. Evaluation of Stream and Wetland Restoration Using UAS-Based Thermal Infrared Mapping. *Water* **2019**, *11*, 1568. [CrossRef]
161. Casas-Mulet, R.; Pander, J.; Ryu, D.; Stewardson, M.J.; Geist, J. Unmanned Aerial Vehicle (UAV)-Based Thermal Infra-Red (TIR) and Optical Imagery Reveals Multi-Spatial Scale Controls of Cold-Water Areas Over a Groundwater-Dominated Riverscape. *Front. Environ. Sci.* **2020**, *8*, 1–16. [CrossRef]
162. Rautio, A.; Korkka-Niemi, K.; Salonen, V.-P. *Thermal Infrared Remote Sensing in Assessing Ground/Surface Water Resources Related to the Hannukainen Mining Development Site*; Mine Water and Circular Economy IMWA: Lappeenranta, Finland, 2017.
163. Bandini, F.; Butts, M.; Jacobsen, T.V.; Bauer-Gottwein, P. Water level observations from unmanned aerial vehicles for improving estimates of surface water-groundwater interaction. *Hydrol. Process.* **2017**, *31*, 4371–4383. [CrossRef]
164. Tang, Q.; Schilling, O.S.; Kurtz, W.; Brunner, P.; Vereecken, H.; Franssen, H.-J.H. Simulating Flood-Induced Riverbed Transience Using Unmanned Aerial Vehicles, Physically Based Hydrological Modeling, and the Ensemble Kalman Filter. *Water Resour. Res.* **2018**, *54*, 9342–9363. [CrossRef]
165. Briggs, M.A.; Wang, C.; Day-Lewis, F.D.; Williams, K.H.; Dong, W.; Lane, J.W. Return flows from beaver ponds enhance floodplain-to-river metals exchange in alluvial mountain catchments. *Sci. Total Environ.* **2019**, *685*, 357–369. [CrossRef]
166. Furlan, L.M.; Rosolen, V.; Salles, J.; Moreira, C.A.; Ferreira, M.E.; Bueno, G.T.; Coelho, C.V.D.S.; Mounier, S. Natural superficial water storage and aquifer recharge assessment in Brazilian savanna wetland using unmanned aerial vehicle and geophysical survey. *J. Unmanned Veh. Syst.* **2020**, *8*, 224–244. [CrossRef]
167. Siebert, C.; Mallast, U.; Rödiger, T.; Ionescu, D.; Schwonke, F.; Hall, J.K.; Sade, A.R.; Pohl, T.; Merkel, B. Multiple sensor tracking of submarine groundwater discharge: Concept study along the Dead Sea. In Proceedings of the EGU General Assembly Conference Abstracts, Vienna, Austria, 24 April–2 May 2014; p. 11217.
168. Lee, E.; Yoon, H.; Hyun, S.P.; Burnett, W.C.; Koh, D.; Ha, K.; Kim, D.; Kim, Y.; Kang, K. Unmanned aerial vehicles (UAVs)-based thermal infrared (TIR) mapping, a novel approach to assess groundwater discharge into the coastal zone. *Limnol. Oceanogr. Methods* **2016**, *14*, 725–735. [CrossRef]
169. Rahman, M.M.; McDermid, G.J.; Strack, M.; Lovitt, J. A New Method to Map Groundwater Table in Peatlands Using Unmanned Aerial Vehicles. *Remote Sens.* **2017**, *9*, 1057. [CrossRef]
170. Bandini, F.; Lopez-Tamayo, A.; Merediz-Alonso, G.; Olesen, D.; Jakobsen, J.; Wang, S.; Garcia, M.; Bauer-Gottwein, P. Unmanned aerial vehicle observations of water surface elevation and bathymetry in the cenotes and lagoons of the Yucatan Peninsula, Mexico. *Hydrogeol. J.* **2018**, *26*, 2213–2228. [CrossRef]
171. Allred, B.; Eash, N.; Freeland, R.; Martinez, L.; Wishart, D. Effective and efficient agricultural drainage pipe mapping with UAS thermal infrared imagery: A case study. *Agric. Water Manag.* **2018**, *197*, 132–137. [CrossRef]
172. Kratt, C.; Woo, D.; Johnson, K.; Haagsma, M.; Kumar, P.; Selker, J.; Tyler, S. Field trials to detect drainage pipe networks using thermal and RGB data from unmanned aircraft. *Agric. Water Manag.* **2020**, *229*, 105895. [CrossRef]
173. Levy, M.C.; Neely, W.R.; Borsa, A.A.; Burney, J.A. Fine-scale spatiotemporal variation in subsidence across California's San Joaquin Valley explained by groundwater demand. *Environ. Res. Lett.* **2020**, *15*, 104083. [CrossRef]

174. Nayyeri, M.; Hosseini, S.A.; Javadi, S.; Sharafati, A. Spatial Differentiation Characteristics of Groundwater Stress Index and its Relation to Land Use and Subsidence in the Varamin Plain, Iran. *Nat. Resour. Res.* **2021**, *30*, 339–357. [CrossRef]
175. Yu, H.; Gong, H.; Chen, B.; Liu, K.; Gao, M. Analysis of the influence of groundwater on land subsidence in Beijing based on the geographical weighted regression (GWR) model. *Sci. Total Environ.* **2020**, *738*, 139405. [CrossRef]
176. Carlson, G.; Carnes, L.K.; Cook, J.P. Exploring Arizona earth fissures: An anthropogenic geologic hazard. *GSA Annu. Meet. Phoenix Ariz.* **2019**, *55*, 115–126. [CrossRef]
177. Hu, X.; Li, X. Information extraction of subsided cultivated land in high-groundwater-level coal mines based on unmanned aerial vehicle visible bands. *Environ. Earth Sci.* **2019**, *78*. [CrossRef]
178. Hu, X.; Li, X.; Min, X.; Niu, B. Optimal scale extraction of farmland in coal mining areas with high groundwater levels based on visible light images from an unmanned aerial vehicle (UAV). *Earth Sci. Inform.* **2020**, *13*, 1151–1162. [CrossRef]
179. Commission Implementing Regulation (EU) 2019/947 of 24 May 2019 on the Rules and Procedures for the Operation of Unmanned Aircraft. Available online: http://data.europa.eu/eli/reg_impl/2019/947/oj (accessed on 30 November 2020).